RadioGraphics

From the Archives of the AFIP

Child Abuse: Radiologic-Pathologic Correlation[1]

CME FEATURE

See accompanying test at http://www.rsna.org/education/rg_cme.html

LEARNING OBJECTIVES FOR TEST 1

After reading this article and taking the test, the reader will be able to:

- Describe the common injury patterns in abused children.
- Recognize the imaging features of inflicted metaphyseal and rib fracture, interhemispheric hemorrhage, and hollow organ abdominal injury in children.
- Discuss the biomechanical basis of common abusive injuries.

Gael J. Lonergan, Lt Col, USAF MC • Andrew M. Baker, MD
Mitchel K. Morey, MD • Steven C. Boos, Lt Col, USAF MC

In the United States, roughly one of every 100 children is subjected to some form of neglect or abuse; inflicted injury is responsible for approximately 1,200 deaths per year. Child physical abuse may manifest as virtually any injury pattern known to medicine. Some of the injuries observed in battered children are relatively unique to this population (especially when observed in infants) and therefore are highly suggestive of nonaccidental, or inflicted, injury. Worrisome injuries include rib fracture, metaphyseal fracture, interhemispheric extraaxial hemorrhage, shear-type brain injury, vertebral compression fracture, and small bowel hematoma and laceration. As noted, however, virtually any injury may be inflicted; therefore, careful consideration of the nature of the injury, the developmental capabilities of the child, and the given history are crucial to determine the likelihood that an injury was inflicted. The majority of these injuries are readily detectable at imaging, and radiologic examination forms the mainstay of evaluation of child physical abuse. Detection of metaphyseal fracture (regarded as the most specific radiographically detectable injury in abuse) depends on high-quality, small field-of-view radiographs. The injury manifests radiographically as a lucent area within the subphyseal metaphysis, extending completely or partially across the metaphysis, roughly perpendicular to the long axis of the bone. Acute rib fractures (which in infants are strongly correlated with abuse) appear as linear lucent areas. They may be difficult to discern when acute; thus, follow-up radiography increases detection of these fractures. For skull injuries, radiography is best for detecting fractures, but computed tomography and magnetic resonance imaging best depict intracranial injury.

Abbreviations: βAPP = beta amyloid precursor protein, CML = classic metaphyseal lesion, NAHI = nonaccidental head injury, SAH = subarachnoid hemorrhage, SDH = subdural hemorrhage, Tc-MDP = technetium-99m methylene diphosphonate

Index terms: Abdomen, injuries, 70.419 • Children, injuries • Extremities, injuries, 40.4195 • Infants, injuries • Head, injuries, 10.419, 10.433 • Ribs, fractures, 471.4195

RadioGraphics 2003; 23:811–845 • **Published online** 10.1148/rg.234035030

[1]From the Department of Radiologic Pathology, Armed Forces Institute of Pathology, 14th and Alaska Sts NW, Bldg 54, Rm M-121, Washington, DC 20306-6000 (G.J.L.); Department of Radiology and Nuclear Medicine, Uniformed Services University of the Health Sciences, Bethesda, Md (G.J.L.); Hennepin County Medical Examiner's Office, Minneapolis, Minn (A.M.B., M.K.M.); and Armed Forces Center for Child Protection, National Naval Medical Center, Bethesda, Md (S.C.B.). Received February 10, 2003; revision requested March 24 and received March 31; accepted April 4. **Address correspondence to** G.J.L. (e-mail: *glonergan@mac.com*).

The opinions and assertions contained herein are the private views of the authors and are not to be construed as official nor as reflecting the views of the Departments of the Air Force, Navy, Army, or Defense.

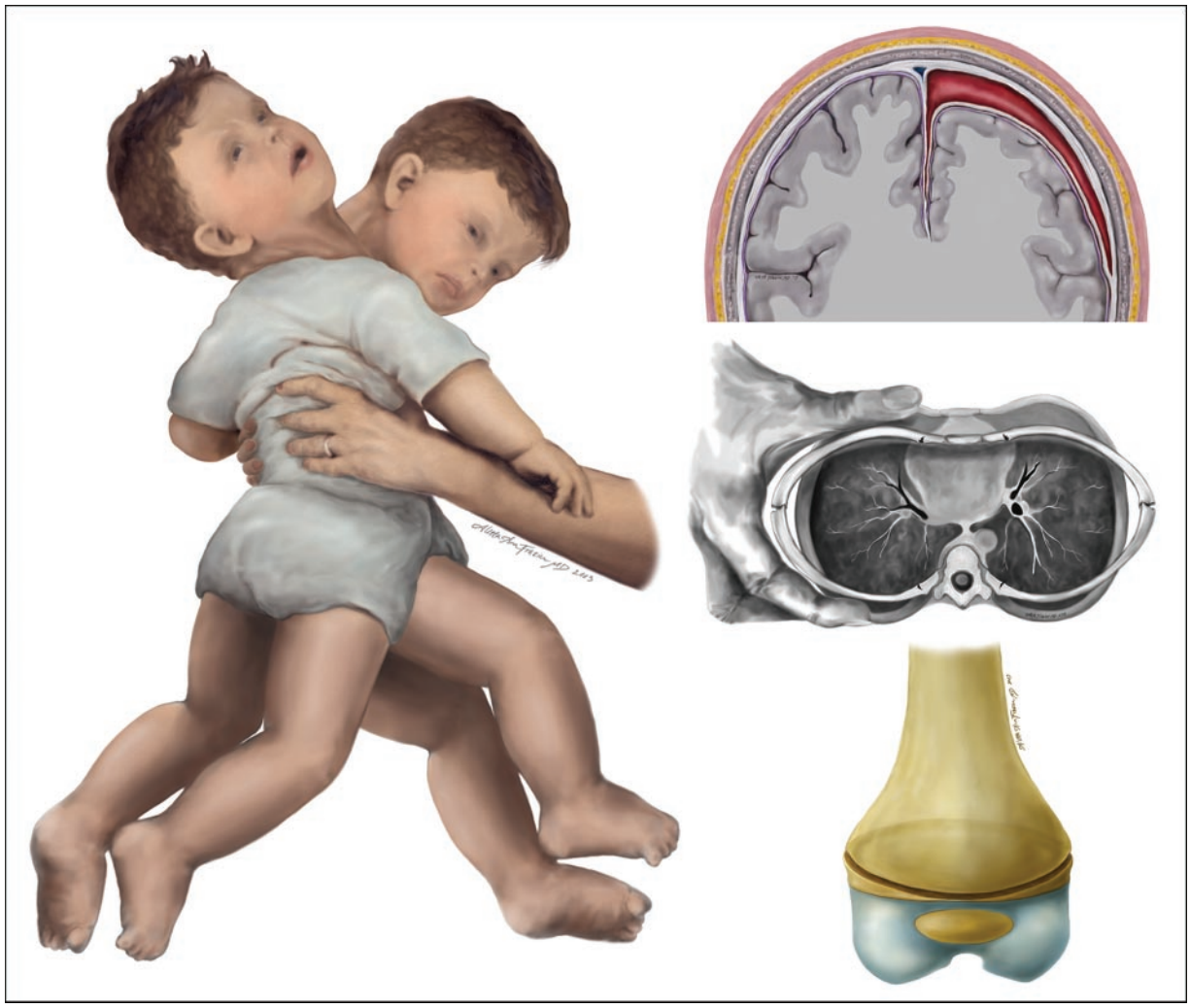

Figure 1. Violent shaking and squeezing of an infant may result in subdural hemorrhage (top right diagram) and shear-type brain injury, rib fracture (middle right diagram), and metaphyseal fracture (lower right diagram). These injuries are fully described and illustrated in subsequent sections.

Introduction

The intentional infliction of pain and suffering, both physical and emotional, on children is a distressingly common occurrence. Harm by caretakers may be categorized as neglect (63% of cases), physical abuse (19%), sexual abuse (10%), and psychologic abuse (8%). In the United States in the year 2000, approximately 1,200 children died as a result of inflicted trauma or neglect, representing a rate of 1.7 per 100,000 children. The youngest children are the most vulnerable: Children less than 1 year of age account for 44% of all abuse-related fatalities. Three million cases of suspected abuse were reported in 2000; 879,000 of these cases were substantiated, representing 1.22% of U.S. children. Parents accounted for 77% of perpetrators (1).

The rate of victimization decreases as age increases: From birth to 3 years of age, 15.7 per 1,000 children are abused or neglected, compared with 5.7 per 1,000 for the 16–17-year-old group. Girls are abused slightly more often than boys when all forms of abuse are considered together (12.8 vs 11.2 for girls and boys, respectively, per 1,000 children). However, in the subcategory of child sexual abuse, girls are more than four times as likely to be victims than boys (1.7 vs 0.4, respectively, per 1,000 children) (1). Physicians and other allied health professionals are mandated by law in all 50 states and the District of Columbia to report suspected abuse within 48 hours to Children's Protective Services (2).

The first description of child physical abuse was by the French forensic physician Ambrose Tardieu (3) in 1860. The next mention in the medical literature was not until 1946, when the American pediatric radiologist John Caffey (4) described six infants with long bone fractures and subdural hematomas. He postulated that these injuries were inflicted and later (1957) described the metaphyseal fracture, which remains to this day the most specific injury in child abuse (5). Kempe et al (6) in 1962 coined the term *battered*

Figure 2. Femoral shaft fracture in an abused 5-year-old boy. Frontal radiograph shows a transverse fracture of the diaphysis in femoral pin traction. The mother's boyfriend confessed to pushing a television cabinet on top of the boy.

child syndrome to describe metaphyseal fracture and other injuries typical of abuse. In 1971, Guthkelch (7) was the first to invoke shaking as the causative mechanism in abusive head injury. Paul Kleinman and colleagues (8–17), beginning in the 1980s and continuing today, have contributed extensively to our understanding of the pathophysiology and mechanisms of injury in child physical abuse. This article reviews the injuries commonly observed in child physical abuse, with special emphasis on those injuries that are highly specific or suggestive of abuse (Fig 1). We discuss the radiologic injury patterns commonly discovered in physically abused children, with special emphasis on the biomechanical forces that produce the injuries, their pathologic and radiologic appearances, and forensic implications of certain features (such as evidence of fracture healing) of the injuries.

Skeletal Injury

Skeletal injury is the most common abuse-related injury (excluding pure soft-tissue injuries such as bruising). Virtually every type and location of fracture has been documented in abused children. The prevalence of fracture varies with report and the population studied. Fracture is documented in 11%–55% of physically abused children (18–20). In one large series of abuse-related fractures (429 fractures), when all pediatric age groups were considered together, 76% of fractures were in the long bones (Fig 2); 8%, the skull; and 8%, the rib cage (21).

Children less than 18 months of age sustain some unusual injuries because of their immature skeletons and unique mechanisms of injury (such as violent shaking). Metaphyseal and rib fractures, in particular, are rarely found in older children with abuse-related injury, but when discovered in infants, these fractures are highly specific for abuse. Thus, the low frequency of these lesions in large fracture series belies their common occurrence in infants. In studies of fracture patterns in infants, rib fractures constitute 35%–60% of fractures (9,22). Although long bone shaft fractures are often seen in abused infants, metaphyseal fractures are the most common long bone fracture in this population. Postmortem specimen radiographic studies of infants yield significantly increased detection of rib fracture; in this population, rib fractures are more common than long bone fractures of any type (9).

Metaphyseal Fracture

Of all the injuries observed in child physical abuse, none is more specific than the metaphyseal fracture. First described in 1957 by the eminent pediatric radiologist John Caffey (5), metaphyseal fracture is virtually pathognomonic of abuse (8). Kleinman et al (9,12–15) coined the term *classic metaphyseal lesion* (CML) to describe the injury. CMLs are relatively common in abused infants and are discovered in 39%–50% of abused children less than 18 months of age (9,22). Thus, CMLs are highly specific for abuse, although they are observed in half or fewer of cases. Overall, CMLs most often occur in the distal femur, proximal tibia, distal tibia, and proximal humerus (8,12–15,22). They are seen almost exclusively in children less than 2 years of age for reasons detailed in the following biomechanical discussion.

The CML is a series of microfractures across the metaphysis; the fracture line is oriented essentially parallel to the physis, although it may not travel the entire width of the bone (8). Its orientation perpendicular to the long axis of the bone reveals that the precipitating force is a shearing injury across the bone end. Shearing in this manner is a peculiar force for a long bone to sustain, since it is the result of differential horizontal motion across the metaphysis and is therefore not a

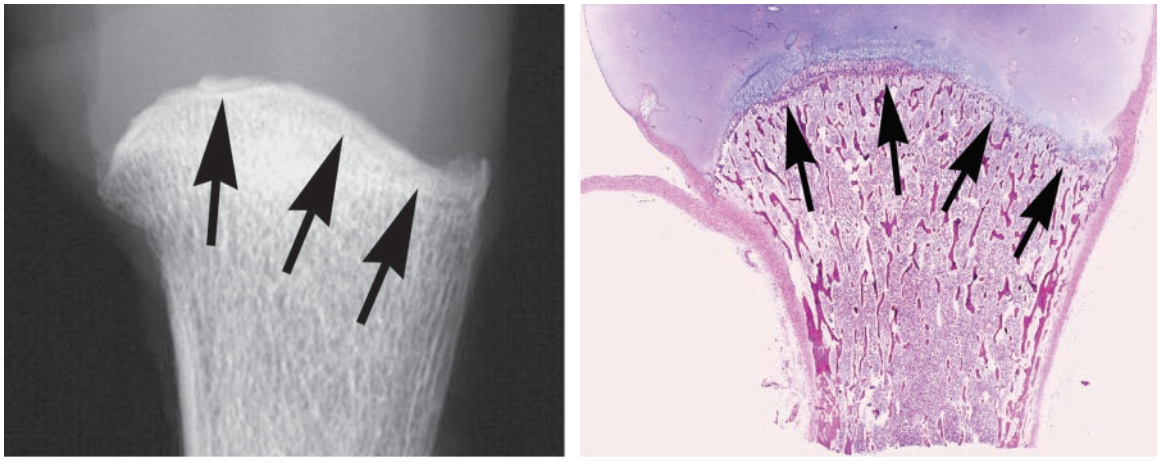

a. b.

Figure 4. Acute CML in a fatally abused 2-month-old child. **(a)** Specimen radiograph of the proximal left humerus shows the subtle lucency of the CML (arrows). **(b)** Photomicrograph (unmagnified, hematoxylin-eosin stain) shows disruption of the calcified cartilage cores of the primary spongiosa (arrows). (Case courtesy of Paul K. Kleinman, MD, The Children's Hospital, Boston, Mass.)

feature of falls or blunt trauma (23,24). The force is generated by manual to-and-fro manipulation of the extremities (eg, holding and shaking an infant by the feet or hands or shaking the infant while he is held around the chest, with the limbs whiplashing back and forth and sustaining horizontal shear forces) (8). Therefore, CML is seen almost exclusively in children less than 2 years of age—those children who are small enough to be shaken violently and who are unable to protect their extremities (24,25). Fortunately, the long-term sequelae of CML appear to be minimal (26).

Pathologic Characteristics.—The elegant work of Kleinman and colleagues in the 1980s established the histologic definition of the CML as a series of microfractures in the subepiphyseal region of bone. This region is the primary spongiosa, and it is the most immature area of the mineralized matrix in the growing metaphysis. Interestingly, it is this immature mineralized bone, and not the adjacent cartilaginous physis, that is disrupted by shearing forces. Microfractures extend variably across the metaphysis and may completely or partially traverse it. When complete, the fracture fragment may be conceptualized as a wafer or disk of bone (primary spongiosa), separated from the shaft by the series of metaphyseal microfractures (Fig 3). The edge (rim) of the CML tends to be thicker than its center, since at the periphery the microfractures usually angle obliquely toward the diaphysis, thus creating a rim of relatively thicker bone at the periphery of the disk-shaped fracture fragment. The more central microfractures are closer to the physis, resulting in a considerably thinner central region of the fracture fragment. The CML, when complete, is a disk with a broad, thin center and a thick circumferential rim (8).

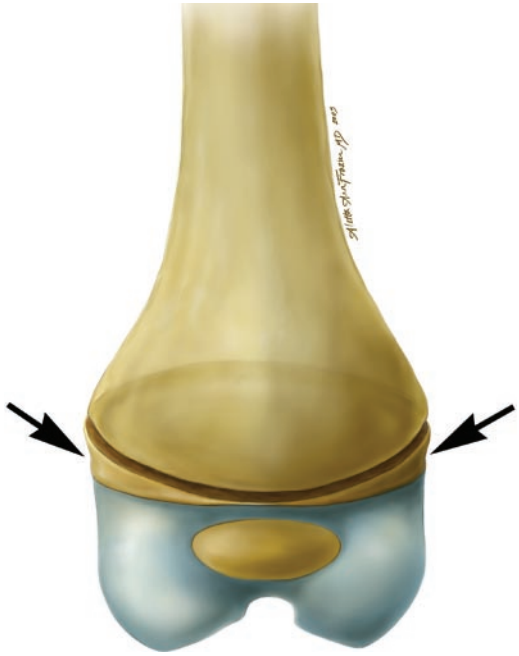

Figure 3. Diagram depicts the discoid metaphyseal fracture fragment (arrows).

Acute CML manifests as disruption of the bony trabeculae in the primary spongiosa (Fig 4). The columns of calcified cartilage extending into the metaphysis are also disrupted. Periosteal disruption and extension into the physis are relatively rare (8). When the acute CML heals, there is an increase in the number of regional osteoblasts and osteoclasts, as well as fibrin deposition.

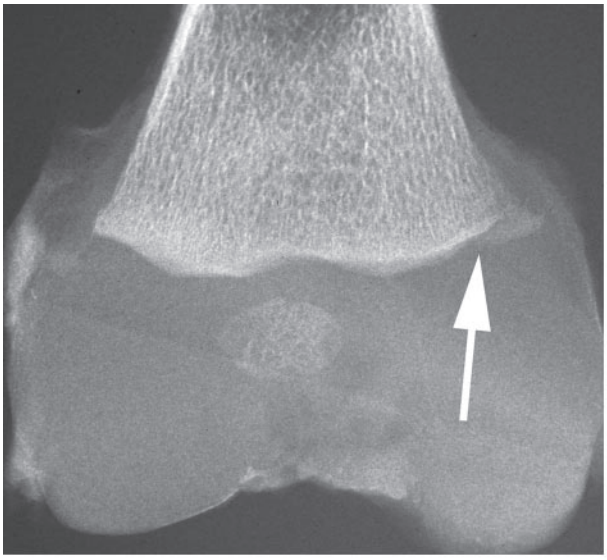

a.

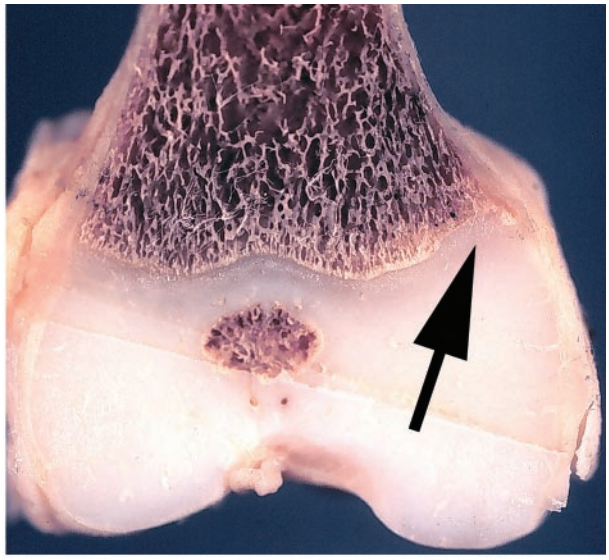

b.

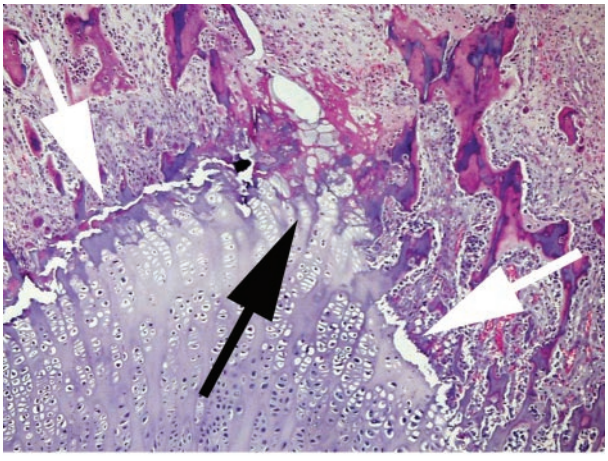

c.

Figure 5. Subacute CML in a fatally abused 7-week-old boy. **(a)** Specimen radiograph of the distal femur (overlying soft tissue removed) shows irregular lucency of the medial femoral metaphysis (arrow). **(b)** Photograph of the fixed, bivalved femur shows physeal cartilage extension into the metaphysis (arrow). **(c)** High-power photomicrograph (original magnification, ×100; hematoxylin-eosin stain) of the physis reveals hypertrophied chondrocytes (black arrow) growing into the metaphyseal fracture site (white arrows).

There is typically no periosteal disruption, and little or no callus is formed. However, changes at the physis subjacent to a CML may indicate a subacute CML.

A review of normal longitudinal bone growth at the physis will help clarify the discussion of the subacute CML. The normal physis (the cartilaginous growth plate situated between the epiphysis and metaphysis) is a disk of chondrocytes that extends in columns toward the metaphysis. With growth, the juxtametaphyseal chondrocytes (which form the hypertrophic zone of the physeal cartilage) die, and mineralization of the osteoid around the cartilage columns occurs. Thus, there is progressive mineralization of the hypertrophic (juxtametaphyseal) zone of the physis, such that longitudinal bone growth proceeds at the metaphysis. This pattern of metaphyseal growth depends in part on a normal vascular supply to the hypertrophic zone of physeal cartilage, which is derived from the metaphysis (27). Studies have shown that disruption of the vascular supply leads to an abnormally thick physis, representing diminished mineralization at the chondroosseous junction (28). Similar changes at the chondroosseous (physeal-metaphyseal) junction have been observed in the CML, occurring distal to, not within, the metaphyseal injury. It is believed that the CML disrupts blood supply to the more distal metaphyseal fragment and its neighboring hypertrophic zone, resulting in persistence of the hypertrophic zone and diminished matrix mineralization. Thus, unaffected regions of the metaphysis-physis complex grow and mineralize normally around the injured area; however, the area distal to the CML does not mineralize normally, and the chondrocytes persist abnormally. At histologic analysis, this pattern appears as an area of focal or diffuse (depending on the extent of the CML) hypertrophic chondrocyte columns in the primary spongiosa (Fig 5) (10). One study found this pattern in 15 of 15 healing CMLs; in the same study, only one of 25 fractures in which this

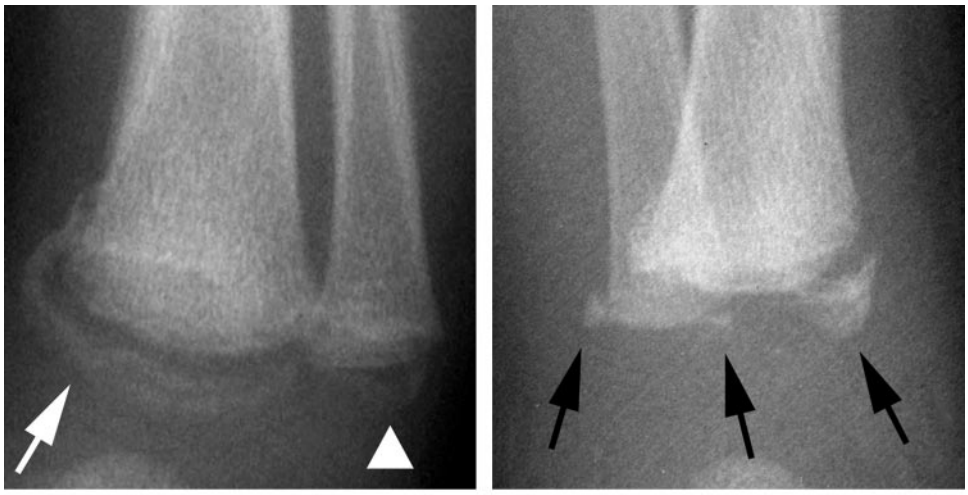

a. b.

Figure 6. CML in an abused 2-month-old girl. **(a)** Frontal radiograph of the ankle shows a rim of bone (arrow) separated from the tibial shaft by the metaphyseal fracture lucency, giving the appearance of a bucket handle. A CML of the distal fibula is also faintly seen (arrowhead). **(b)** Lateral radiograph depicts the tibial and fibular fractures as corner fractures (arrows).

finding was missing demonstrated evidence of healing. No acute fractures in this study showed physeal cartilage extension into the metaphysis (29). The extension of hypertrophic cartilage into the primary spongiosa is an excellent indicator of a subacute CML.

Radiologic Appearance.—The radiologic appearance of the CML correlates very closely with its histologic counterpart. It manifests as a lucent area within the subphyseal metaphysis, extending completely or partially across the metaphysis, roughly perpendicular to the long axis of bone. Because the wafer of bone that is the fracture fragment may have a very thin center, this region may be radiographically occult. The thicker peripheral rim is more readily visible and appears as a triangular fragment when viewed in profile (commonly referred to as a corner fracture). If the fragment is separated from the remainder of the long bone by a prominent fracture lucency, or if the fracture is viewed at a slightly oblique angle, the thick rim may be visible as a curvilinear structure resembling a bucket handle (Fig 6). Thus, the appearance varies with the length and width of the fracture fragment (ie, how far across with metaphysis the fracture extends), as well as its position at radiography (8). Healing of CML is often difficult to assess, because callus and subperiosteal new bone formation are both unusual. Focal or diffuse extension of the physeal cartilage into the metaphysis, manifested as metaphyseal lucency, is a highly specific indicator of healing, although exact estimation of fracture age cannot be determined from this finding alone (Fig 5) (29).

Skeletal scintigraphy may demonstrate increased uptake of technetium-99m methylene diphosphonate (Tc-MDP) at the CML (Fig 7). However, this finding may be subtle, especially if the examination is not of technically excellent quality and the reader is not experienced in pediatric scintigraphic interpretation. Normal young children may exhibit intense uptake of Tc-MDP at the metaphyses, making it difficult to recognize abnormally increased uptake, especially if it is bilateral. Conway et al and others, in a report of two studies and review of the literature, conclude that skeletal scintigraphy is best conceived as complementary in the evaluation of suspected child abuse (24,30). The American Academy of Pediatrics Section on Radiology reached a similar conclusion in a recent recommendation (31). Scintigraphy is superior, however, to plain radiography for the detection of some injuries, particularly rib fracture.

Rib Fracture

Rib fractures occur in older children and adults as a result of trauma such as falls and motor vehicle accidents. In infants without metabolic bone disease, however, they are distinctly unusual injuries outside the setting of abuse (32–34). In part, this reflects the plasticity of the young child's skeleton and rib cage, which allows the skeletal structures to deform (rather than break) until a threshold is met. Rib fractures in infants are strongly corre-

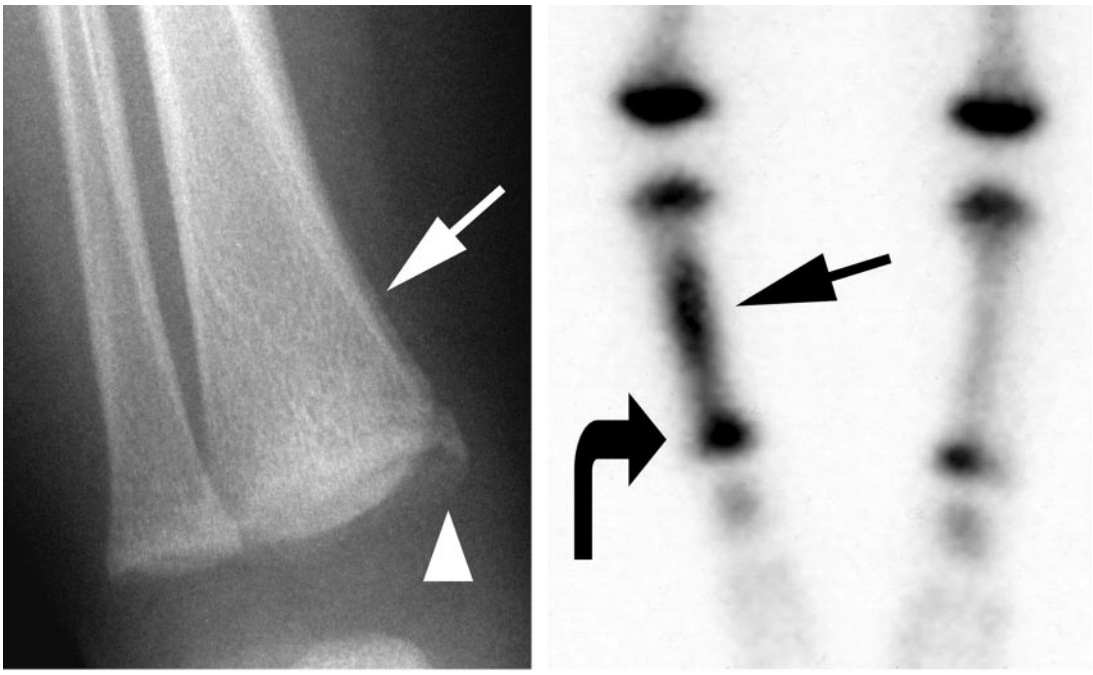

a. b.

Figure 7. Tibial CML in an abused 10-week-old girl. **(a)** Frontal radiograph demonstrates a CML, which has a corner fracture appearance (arrowhead). There is subtle periosteal new bone along the medial tibial shaft (arrow). **(b)** Tc-MDP scan of the lower extremities demonstrates increased uptake along the right tibial shaft (straight arrow) and metaphysis (curved arrow).

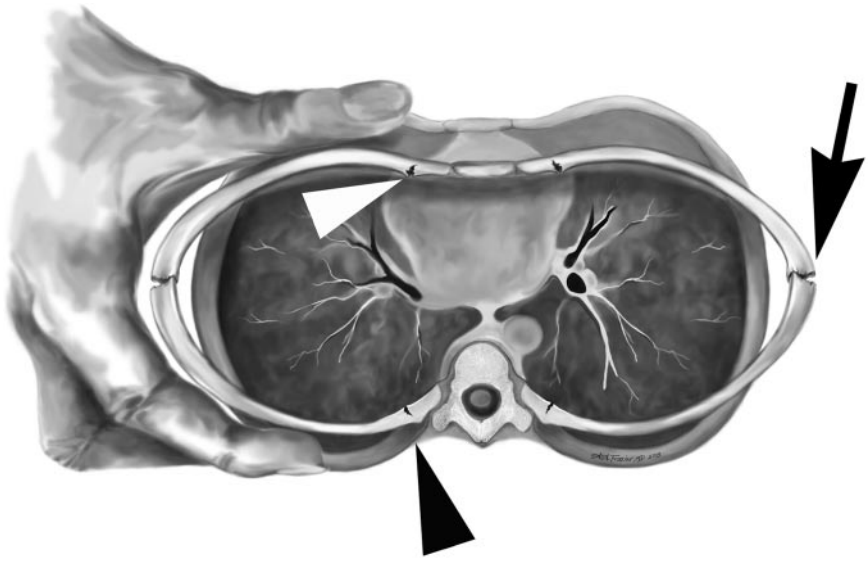

Figure 8. Rib fracture mechanism in tight squeezing. Diagram of the midthorax during tight squeezing reveals anteroposterior compression, which causes compression and fracture of the ribs laterally (arrow). There is hyperextension of the posterior rib ends over the transverse process, with fracture of the ventral cortex (black arrowhead). Anteriorly, the chest wall compression leads to inward bending of the anterior ribs and fracture (white arrowhead).

lated with abuse because the mechanism that generates the fractures is relatively specific. A very tight hold around the infant chest by adult hands generates substantial squeezing force on the immature skeleton and may result in fractures of the anterior, lateral, and posterior aspects of the rib (35,36). Fractures of the first rib are considered virtually diagnostic of child abuse, since they require considerable force (37). In rare cases, rib fracture (including posterior rib fracture) may be produced by birth trauma (38,39). All reported birth-related rib fractures to date have been documented in large babies (>3,300 g), difficult deliveries, or both. Of note, one study of 34,946 live births found no rib fractures (40). Thus, birth-related rib fracture is a rare but reported event.

The rib cage is a roughly tubular structure, with 12 paired ribs attached posteriorly to the spine. When an infant is abusively squeezed around the chest, different mechanical forces are exerted on different parts of the rib cage (Fig 8).

Figure 9. Acute posterior rib fracture in a fatally abused 7-month-old boy. **(a)** Autopsy photograph of the ventral surfaces of the right posterior ribs, after the pleura has been removed, clearly shows the acute rib fractures (arrows). **(b)** Axial specimen radiograph of one of the injured ribs with its vertebral articulations intact shows that the fracture (arrow) is limited to the ventral cortex. (The anomaly of the vertebral arch is an artifact incurred during autopsy resection.) **(c)** In an axial photomicrograph (unmagnified, hematoxylin-eosin stain) of one of the injured ribs with its vertebral articulations intact, the fracture is clearly visible (arrow), as is the cartilage of the rib head (*) and rib tubercle (♦).

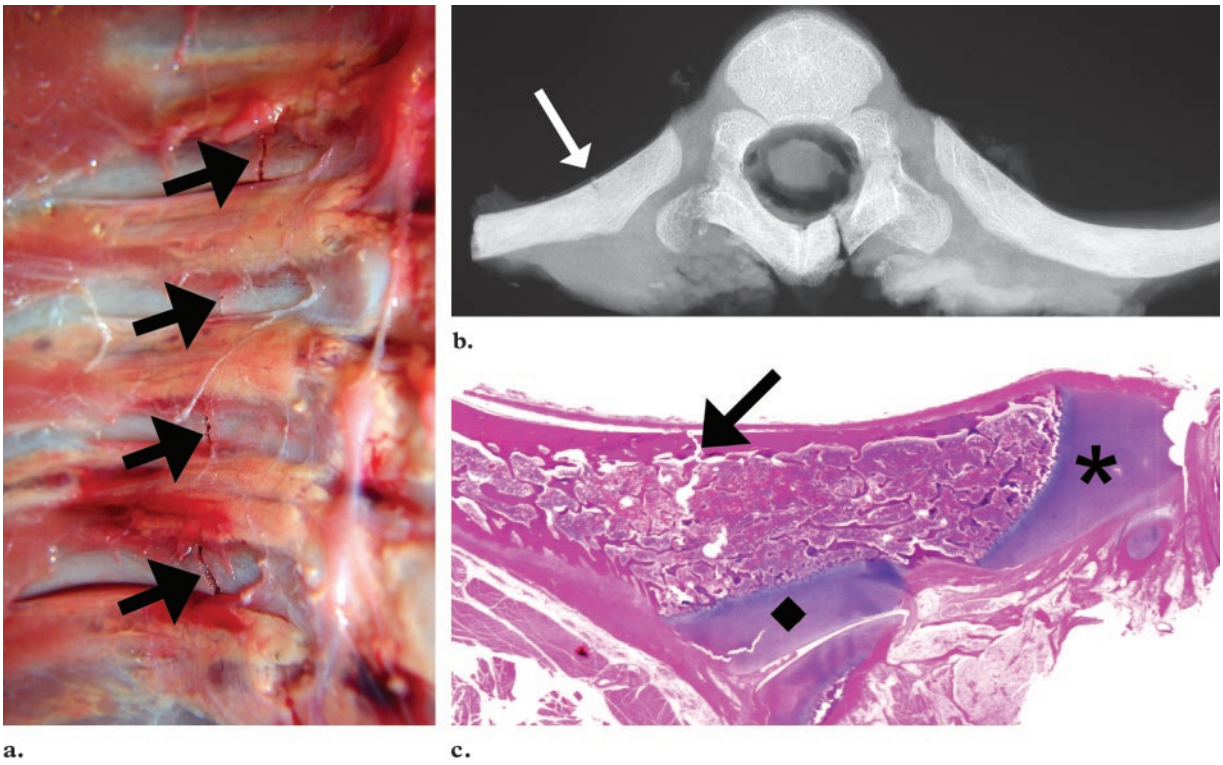

Posteriorly, the ribs are attached relatively tightly to the vertebral bodies and transverse processes; as the posterior rib arcs are squeezed, the posterior rib arc is levered over the transverse process, resulting in ventral (and sometimes complete) cortical disruption (41–44). This levering action is unusual; it is not a feature of most traumatic and iatrogenic (eg, cardiopulmonary resuscitation) forces. For this reason, posterior rib fracture in particular is highly specific for inflicted trauma. Laterally, squeezing creates both anterior and posterior compressive forces, resulting in buckling and impaction of the inner cortex and distraction of the outer cortical fracture margins (44). At the costochondral junction, sternal compression produces inward bending of the costochondral junction, also leading to fracture (44). Thus, tight squeezing of the infant's chest results in a complex array of compressive and levering forces that leads to fractures of the posterior, lateral, and anterior rib. Because the forces are distributed in an area similar to the size of the perpetrator's hands, fractures are typically seen in similar locations in multiple adjacent ribs and are often bilateral.

Pathologic Characteristics.—Acute fractures of the rib are characterized by disruption of the cortex and subjacent bony trabeculae (Fig 9). Hemorrhage is often observed at the fracture site; the periosteum may be intact or disrupted. Fracture healing rapidly ensues and may be divided into four stages: inflammation, soft callus (also called reparative), hard callus, and remodeling. Initially, an intense inflammatory response is elicited by the necrotic bone ends at the fracture site. Cells delivered by blood vessels (predominantly in the periosteum) enter the hematoma, which serves mainly as a scaffold for the repair process (45). The invading cells produce fibrous tissue, cartilage, and finally immature (woven) bone (Fig 10). The soft callus phase of repair is heralded by the appearance of woven bone and cartilage. The woven bone will remodel into mature lamellar

Figure 10. Acute lateral and healing posterior rib fractures in a fatally smothered 7-week-old boy. **(a)** Frontal chest radiograph of the deceased infant reveals widening of the posterior right third through eighth ribs (arrows). **(b)** Magnified view of the lower lateral left chest wall reveals fractures of the lateral left seventh and eighth ribs, without callus (arrows). **(c)** Specimen radiograph of the anterolateral part of the left eighth rib reveals a fracture of the inner cortex (arrow). **(d)** Autopsy photograph of the resected chest cage shows the healing posterior rib fractures (arrows), which are subtle but distinctly larger and more bulbous than the contralateral normal posterior ribs. **(e)** Axial specimen radiograph of the right sixth posterior rib clearly shows the fracture callus (arrow). The vertebral articulations and the contralateral left sixth rib in the specimen are intact. **(f)** Axial photomicrograph (unmagnified, hematoxylin-eosin stain) of the rib fracture depicted in **e** shows mineralized callus (arrow).

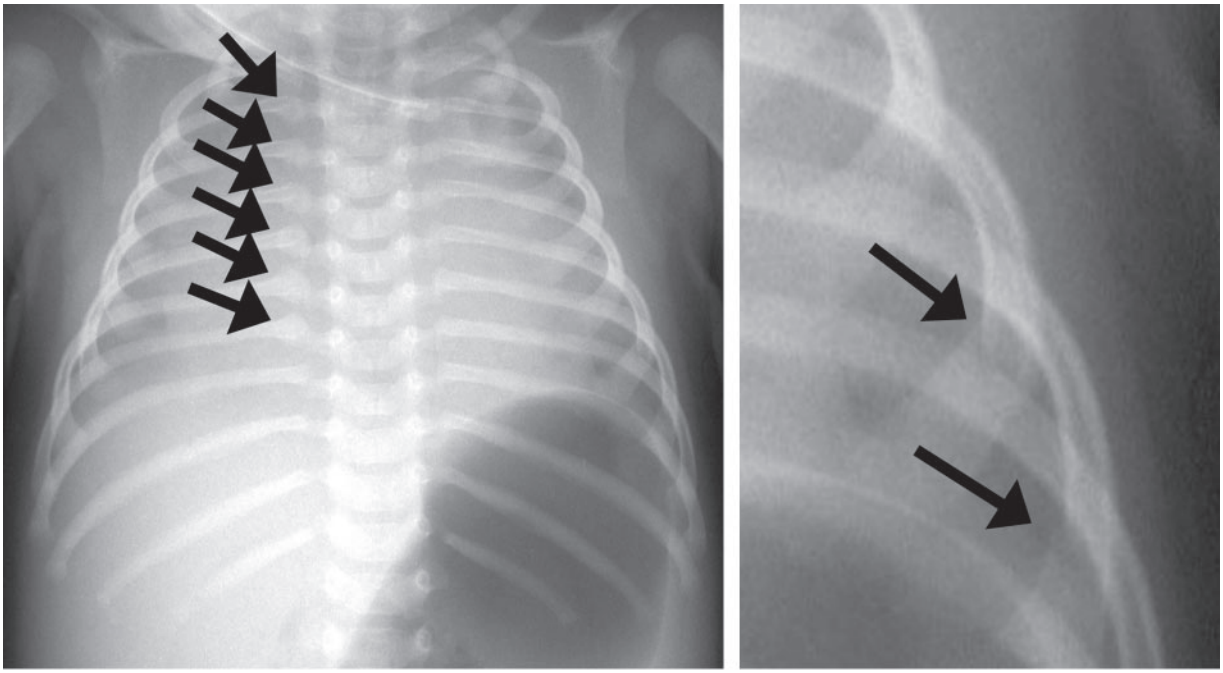

a. b.

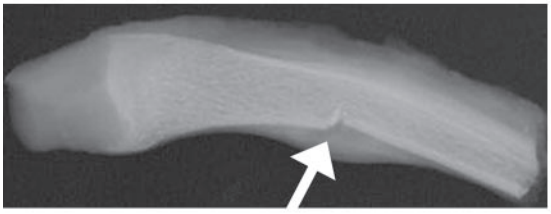

c.

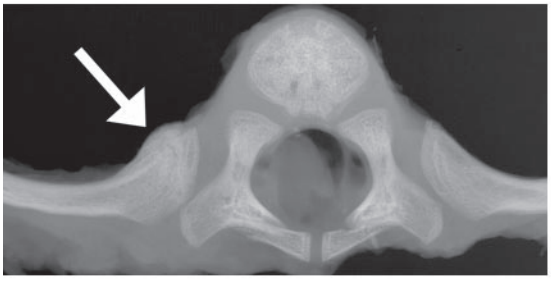

e.

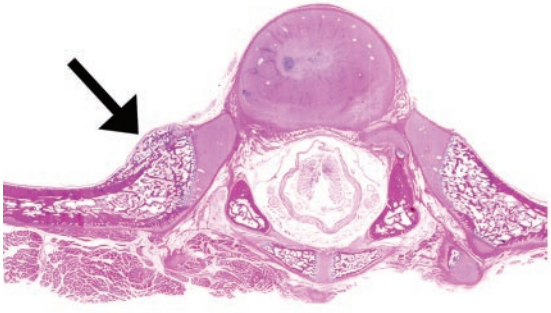

f.

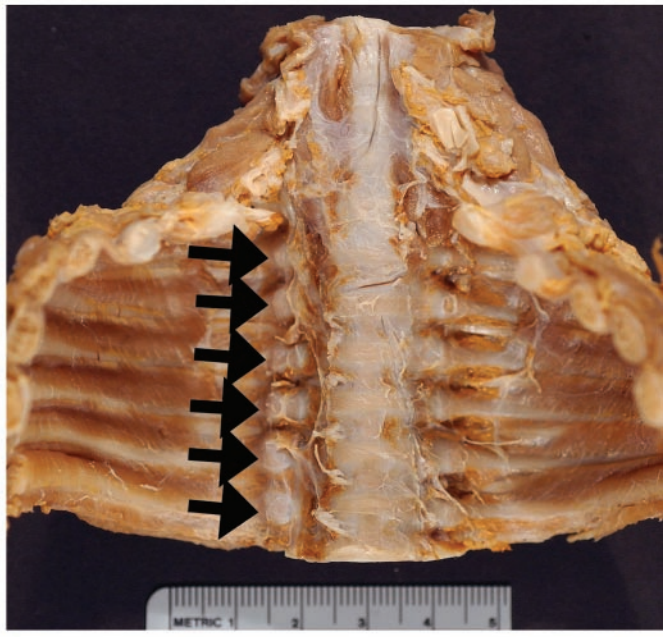

d.

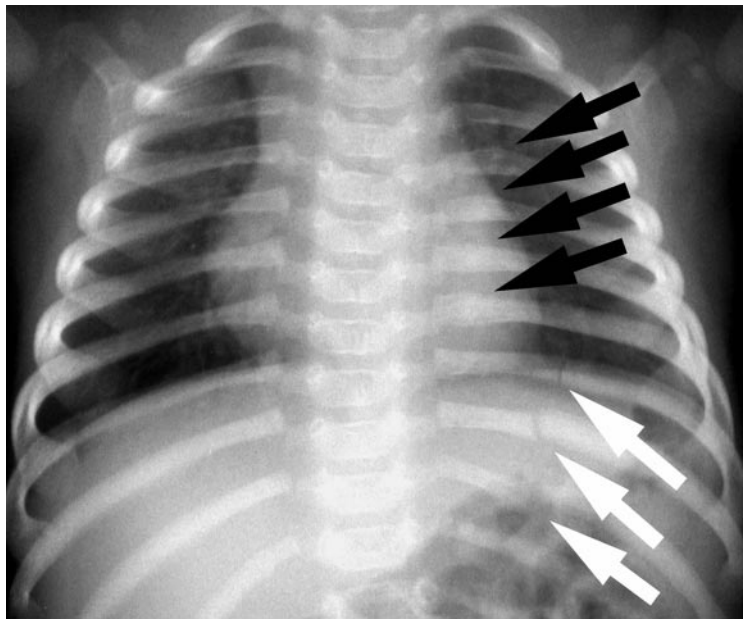

Figure 11. Posterior rib fractures in an abused 3-month-old girl. Frontal chest radiograph reveals fractures without visible callus (white arrows) of the posterior eighth through tenth ribs. The posterior left fourth through seventh ribs are slightly thicker and more opaque than the opposite, normal right posterior ribs, indicating healing posterior rib fractures (black arrows).

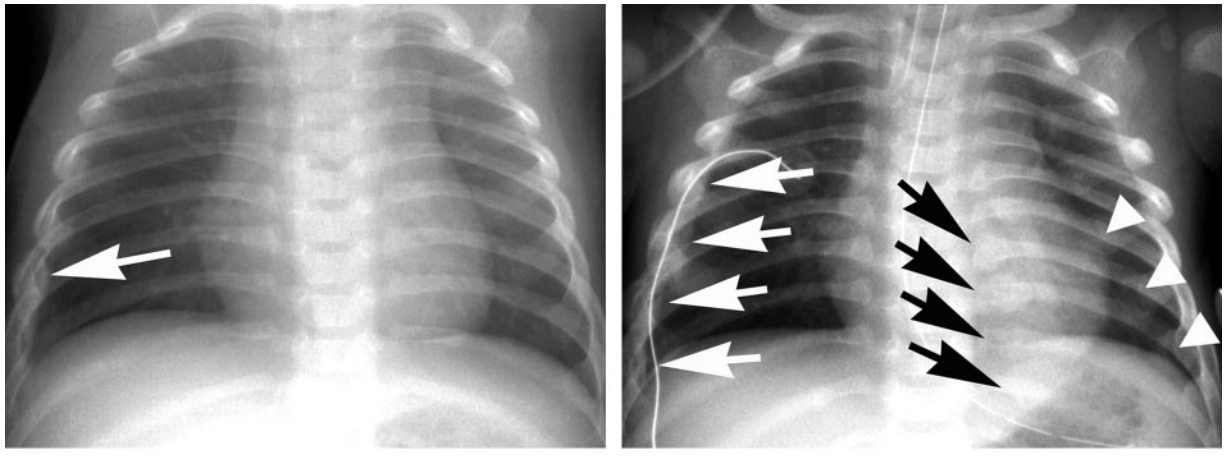

a. **b.**

Figure 12. Increased rib fracture conspicuity over time in an abused 5-month-old boy. **(a)** Frontal chest radiograph obtained at presentation with seizure reveals right lateral sixth rib fracture with callus (arrow) and possibly fractures of the right lateral fourth, fifth, and seventh ribs. **(b)** Frontal chest radiograph obtained 2 weeks later depicts healing right lateral fourth through seventh rib fractures (white arrows). New from comparison is callus of the posterior left seventh through tenth ribs (black arrows). Also noted are fractures of the anterior left fourth through sixth ribs (arrowheads).

bone (hard callus); at this time, the fracture line is bridged by callus and solidly united (46,47). Over the following months (and even years), more trabecular bone will be laid down along stress lines and the marrow cavity will be reconstituted (48, 49). Within different parts of a given fracture, competing inflammatory and callus-forming activities may occur at the same time.

Radiologic Appearance.—Acute rib fractures appear as linear lucent areas (which may be complete or incomplete) across the rib (Fig 11). However, acute rib fractures may be quite difficult to discern, especially if the fracture is incomplete, nondisplaced, or viewed in an area with many superimposed structures or if the fracture line is oblique to the x-ray beam. Fractures of the rib head (at the costovertebral articulation) are particularly difficult to appreciate radiologically for all of these reasons, because they are often superimposed on the transverse process, are nondisplaced, and are oriented obliquely relative to the x-ray beam (41). In a series of 29 posterior rib fractures, only four were clearly visible at high-detail frontal radiography (42). With healing, most fractures become more visible, as subperiosteal new bone and callus become evident (Fig 12). Thus, follow-up radiography performed several weeks after the injury increases detection of

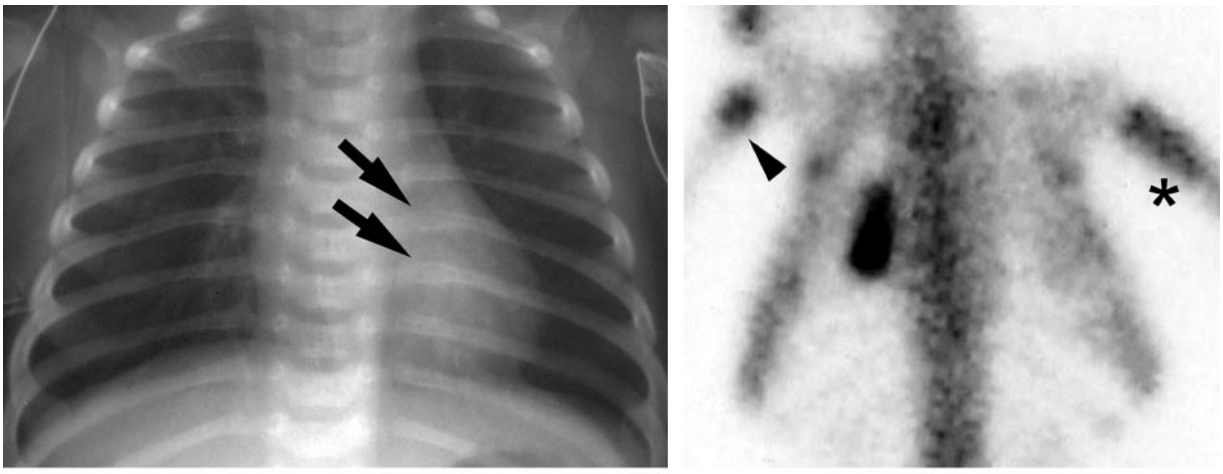

a. b.

Figure 13. Radiographically occult posterior rib fractures detected at bone scintigraphy in an abused 1-month-old boy. **(a)** Frontal chest radiograph reveals subtle increased width of the posterior sixth and seventh ribs (arrows). **(b)** Posterior Tc-99m MDP scan obtained the same day demonstrates increased uptake in multiple adjacent posterior left ribs. Incidentally noted is increased uptake of both proximal humeri, determined at skeletal survey to be secondary to a CML of the left proximal humerus (arrowhead) and periostitis of the right proximal humerus (*).

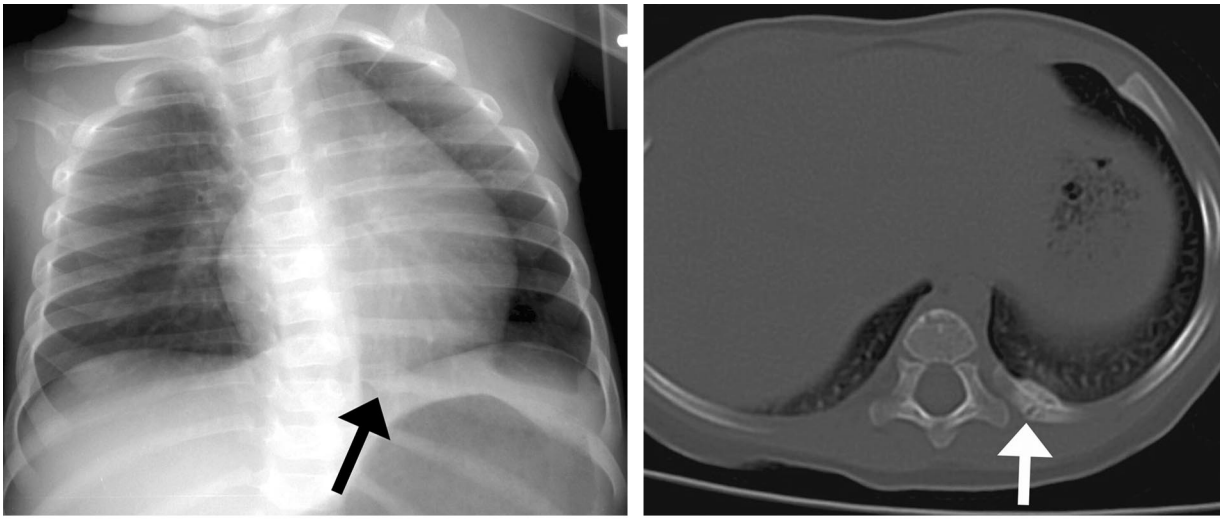

a. b.

Figure 14. Healing posterior rib fracture in an abused 2-month-old girl. **(a)** Frontal chest radiograph shows focal widening of the posterior left ninth rib (arrow). **(b)** Axial CT scan of the chest windowed for bone detail shows the posterior rib fracture with callus (arrow).

rib fracture (50). Fractures involving the anterior and posterior ends of the ribs sometimes have an injury pattern very similar to that of the CML; indeed, the chondroosseous junction of the rib ends is analogous to that of long bones. Callus may not become evident when fractures of the rib occur in these locations, rendering them difficult to see even when healing. Oblique chest radiography (performed with high-detail systems and bone technique) and bone scintigraphy are especially helpful for the improved detection of rib fracture (50). In one study, scintigraphy demonstrated radiographically occult rib fractures in 10% of abused children (51). Other studies confirm that scintigraphy is sensitive for the detection of abuse-related fracture and is a useful adjunct to the radiographic skeletal survey (Fig 13) (30, 52,53). To increase detection of rib fracture, oblique chest radiography, bone scintigraphy, or follow-up chest radiography in 2 weeks is recommended (54). Computed tomography (CT) is a valuable adjunct, although no studies comparing CT with established imaging modalities for the detection of nonaccidental skeletal injury have been reported to date (Fig 14).

Cardiopulmonary Resuscitation and Rib Fracture in Children.—Cardiopulmonary resuscitation (CPR) may result in rib fracture, although fracture is considerably more common in adults than in children receiving CPR (55). Numerous reports in the literature attest to the rarity of CPR-related rib fracture in children. Four series described a total of 446 children who underwent CPR, of whom three had CPR-related rib fracture. Notably, all of these fractures involved the anterior ribs (56–59). The highly specific posterior rib fracture has never been definitively documented to result from CPR. In an experimental study on CPR in rabbits, no posterior rib fractures could be induced, despite vigorous chest compression. Axial CT performed during chest compression helped confirm that levering of the posterior rib over the transverse process does not occur when the back is supported, as it is during CPR (back support limits excursion of the posterior rib arc relative to the spine, therefore limiting levering of the posterior rib head over the transverse process) (43). Thus, posterior rib fracture is highly specific for abuse and does not result from CPR. Not surprisingly, it has never been documented in the scientific literature.

Fracture Healing in Children

The process of fracture healing described in the preceding sections occurs in children as in adults. Questions arise about the age of fractures in abused children, since there may be more than one fracture or the history given may be suspect. Unfortunately, there is little in the literature that aids us in precise dating of fractures in the very young child. One study in infants found that subperiosteal new bone (soft callus) is visible by 10 days after the injury (60). Another study evaluated the radiologic signs of healing of immobilized fractures in children 1–17 years old with known fracture ages. The earliest finding was blurring of the fracture margins, although this was observed in only 60% of fractures (the presence of casting material likely made this difficult to discern in many patients). Periosteal new bone was not observed before 2 weeks but was seen in all at 4 weeks. Visible (calcified) callus was observed in all fractures by 4 weeks and was seen as early as 2 weeks in some cases. Incomplete bridging of the fracture line was noted as early as 3 weeks after injury, and complete bridging (absence of a visible fracture lucency) was evident in almost half (40%) at 10 weeks (61). For a number of reasons, care must be taken when extrapolating these findings and conclusions to infants. Rib fractures are subject to continual motion as a result of breathing and handling; the effect of motion on the radiologic evolution of infant fracture healing is unknown. Infants appear to heal more quickly than do older children and adults (46,47).

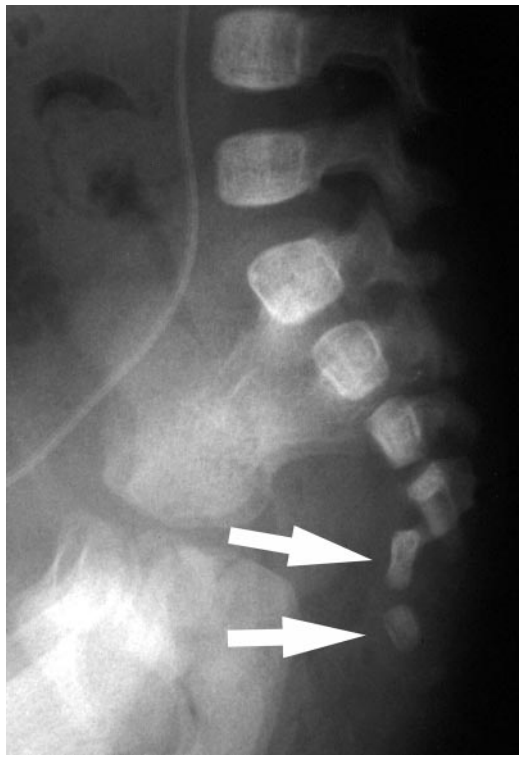

Figure 15. Sacral fracture dislocation in an abused 2-month-old girl. Lateral radiograph depicts a fracture between the fourth and fifth vertebrae, through the intervertebral disk space. The fifth sacral vertebra and coccyx (arrows) are anteriorly displaced. The injury was originally explained as resulting from a changing table fall; the mother's boyfriend later confessed to slamming the child down in a sitting position.

Other Fractures

Virtually every type of fracture has been described in the setting of inflicted trauma. Therefore, any fracture is possibly abusive in origin. Particular attention should be paid to the age and developmental abilities of the injured child as well as to the injury and its mechanism. A 6-week-old child, who cannot yet crawl, is unable to arrive at the top of a flight of stairs and cause his own fall down the stairs. Once a child can walk, he is capable of causing himself considerable harm. The

Figure 16. Spiral femoral fracture in an abused 3-month-old boy. Lateral radiograph shows a displaced, spiral fracture of the femur.

history given for the injury is also extremely important, since it reveals the degree of force and how likely the child was to cause his own injury. Household falls (eg, from a kitchen counter, changing table, sofa, crib, bed) are common accidents, but they are also frequently fabricated as a cause of injury by child abusers attempting to conceal their actions. Household falls infrequently result in fracture or other serious injury (Fig 15). In three separate studies, a total of 529 children sustained falls from heights up to 150 cm (283 of them were witnessed falling onto hard vinyl floors in the hospital). These falls resulted in a total of nine fractures: four skull, four clavicle, and one humerus (62–64). This represents a 1.7% incidence of fracture from household falls.

A fall down stairs is often offered as an explanation for an inflicted injury. It is important to note that although a household staircase will typically traverse 8–10 vertical feet, falls down stairs are not comparable with free falls of that distance. Some have characterized a stairway fall as an initial moderate fall (the initial impact) followed by multiple short falls (subsequent tumbles down adjacent stairs) (65,66). Accordingly, epidemiologic studies of stairway falls demonstrate a limited injury pattern (65,67). Head injury from stairway falls is most commonly seen, followed by extremity injury, and much less often are trunk injuries observed (intestinal perforation has largely been excluded as a possible outcome of simple stairway falls) (68). The injuries are typically mild to moderate, including skull and extremity fracture, concussion and brain contusion, and uncommonly a small subdural hematoma. The occurrence of more than one locus of injury (eg, a femur fracture and a skull fracture) is distinctly unusual. Certain factors can increase the severity of stairway falls, such as falling down stairs from the arms of an adult (which may significantly increase the vertical distance of the initial fall). Falling down stairs while in a walker, however, is considerably more injurious and may result in fatal head injury (69).

Spiral long bone and spine fractures deserve special mention because they are unusual injuries and imply mechanisms of force that are unusual, at least in infants. Spiral fractures wind around a long bone and are the result of torsional forces applied to the bone. Because of this unusual force, they are distinctly uncommon in infants, who typically sustain accidental injury from falls (Fig 16). Unless there is a good accidental explanation, spiral fractures in nonambulatory children are quite suggestive of inflicted injury (70,71). Once a child is walking, spiral fractures of the tibia ("toddler's fracture") are quite common, often have no memorable traumatic antecedent, and by themselves are not suggestive of abuse.

Any spinal fracture without good accidental explanation, especially in an infant, is suggestive of abuse. Thoracolumbar compression fracture may be caused by shaking; when a baby is held around the chest and shaken, there is extension and flexion, centered at the thoracolumbar junction. Compression fracture of lower thoracic and upper lumbar vertebrae may result (with loss of vertebral body height or other compression deformity), as may avulsion of the posterior interspinous ligament at these levels (Fig 17) (17). Injury to the vertebral body is usually readily apparent at radiography irrespective of the age of the injury, because these deformities tend to persist. However, an interspinous ligament avulsion, with avulsion of the spinal apophysis, may be occult initially, since it is a cartilaginous and soft-tissue injury in infants. Over days to weeks, calcification may become evident (72,73).

Postmortem Radiography

Children who die an unexplained or unexpected death normally undergo autopsy to determine the cause and manner of death. A complete forensic autopsy consists of external evaluation for bruises, burns, penetrating injuries, etc. For the internal evaluation, the cranium, thorax, and abdomen (and sometimes neck) are opened and thoroughly inspected. Radiographs may be obtained as part of the autopsy, although they are usually images of large areas of the body or even the whole body of a small child (a "babygram"). Although these images may be adequate to detect a foreign body such as a bullet, they are inadequate for the detection of subtle injuries of abuse such as CML and rib fracture. In addition, the metaphyses are not routinely evaluated at autopsy. Detection of CML (regarded as the most specific, radiographically detectable injury in abuse) depends on high-quality, small field of view radiographs (9,44,74). In the landmark study by Kleinman et al (9) of postmortem radiography, fully 93% of infants had evidence of older, highly abuse-specific injuries detected radiographically. Another study revealed that the findings at postmortem radiography influenced the determination of manner of death for six of eight fatally abused infants (74). For all these reasons, it is imperative that children dying under any suspicious circumstances undergo a skeletal radiographic survey as part of the postmortem evaluation. This survey is most easily accomplished while the child's body is still in the hospital, before it is transported to the medical examiner's office or morgue.

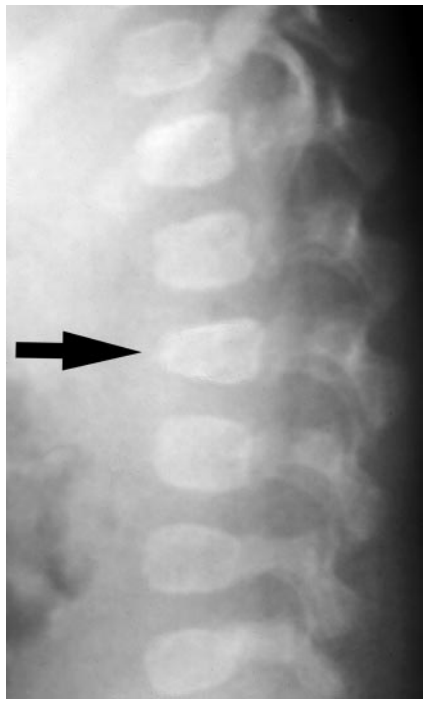

Figure 17. Vertebral body compression fracture in a shaken 3-month-old boy. Lateral radiograph of the lower thoracic and upper lumbar spine reveals anterior wedging of the second lumbar vertebra (arrow).

Central Nervous System Injury

Nonaccidental head injury (NAHI) occurs in approximately 12% of physically abused children and, in children under 2 years of age, accounts for 80% of deaths from head injury (75). In children less than 1 year old, 95% of all serious head injuries and 64% of all head injuries result from abuse (76). The outcome of infants suffering NAHI is considerably worse than for those of the same age who have sustained accidental brain injury (75). NAHI in infants is associated with 12.5%–40% mortality (77–80). Mental retardation and disability are common sequelae of abuse in those infants who survive. In one study of 14 surviving children of infant NAHI, seven (50%) were severely disabled or vegetative, two were moderately disabled, and five had a "good" outcome (although three from this last group repeated grades or needed tutoring) (81). NAHI is the leading cause of morbidity and mortality in abused children.

Skull Fracture

Skull fractures are relatively common in both accidental and abusive injury. In all cases and age groups of abused children, they represent approximately 8%–13% of fractures (21). However, in children less than 2 years of age, the percentage rises to 29%–33%. In abuse-related homicides in infants, skull fracture is discovered in up to 41% of cases (Fig 18) (9). Overall, there is generally poor correlation of skull fracture and underlying hemorrhage or brain injury, and skull fracture is found in children with brain injury in 23%–56% of cases (82–86). It is believed that deformation (inbending) of the infant skull injures the subjacent brain and meninges without fracture.

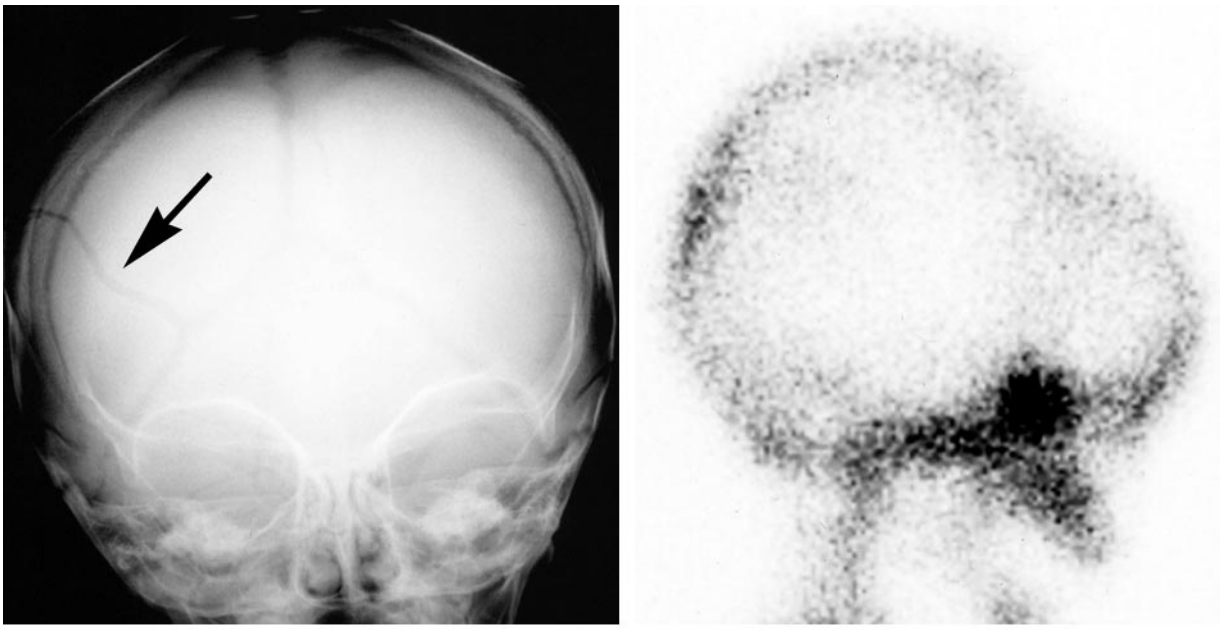

a. b.

Figure 18. Linear parietal skull fracture secondary to abuse. **(a)** Frontal skull radiograph depicts a linear, right parietal skull fracture (arrow). **(b)** Lateral TC-MDP scan of the head appears normal.

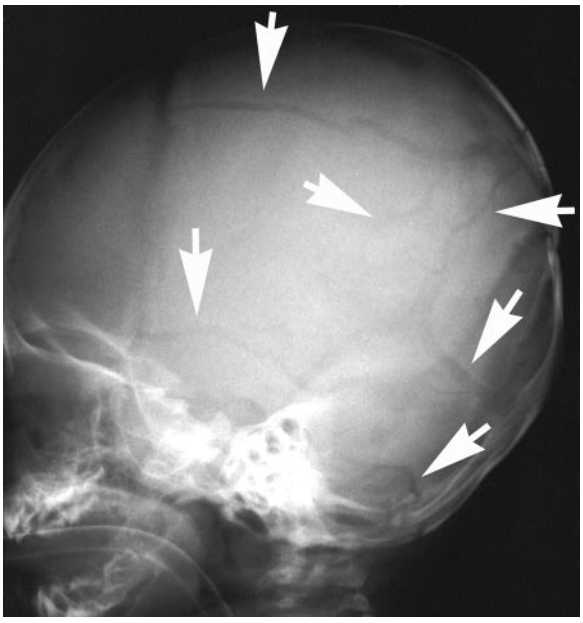

Figure 19. Complex skull fractures in an abused 3-month-old girl. Lateral skull radiograph reveals multiple skull fractures (arrows).

Skull fractures result from contact injury. The velocity of the object striking the skull, or of the skull as it strikes a stationary object (as in a fall), dictates the magnitude of the contact force and thus the likelihood of fracture. The surface area and type of surface contacted influence whether a skull fracture will result: The larger and softer the surface area, the less likely a fracture will occur. A small contact area, given sufficient velocity, will result in a depressed skull fracture. The infant skull is relatively plastic (deformable) and thus tends to be more resistant to fracture. Not surprisingly, studies repeatedly show that skull fractures occur in only 1%–3% of children as a result of short (usually defined as 6 feet or less) falls (62–64,87,88). It is important to note that although skull fractures are not rare in household trauma, significant underlying brain injury (with the exception of epidural hematoma) is rare in household trauma. Only very rarely has severe brain injury and even death been reported from witnessed short falls (63,77,89). Cerebral contusions underlying direct trauma may result from more complex falls, such as stairway and bunk bed falls (67,90,91). Soft-tissue swelling may be absent, even in acute skull fracture; thus, lack of swelling should not be construed as evidence that the fracture is subacute (92–94).

Skull fracture patterns have been investigated to determine if any suggest an abusive cause, and none reliably do so. Studies have demonstrated, however, that multiple fractures, fractures that cross sutures, and bilateral fractures are more likely to be associated with abuse (Fig 19)

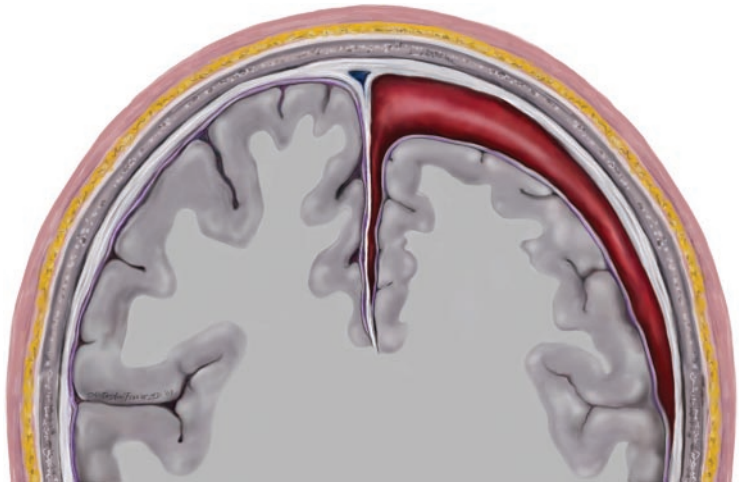

Figure 20. Subdural hemorrhage. Diagram of a coronal view through the brain depicts blood subjacent to the inner dura mater along the left cerebral convexity and adjacent to the interhemispheric falx.

(55,76,84,95,96). Reports vary as to the significance of diastasis; in one report, diastasis greater than 3 mm was associated with inflicted injury (96). Discovery of any fracture for which the history or developmental capabilities of the child are inconsistent should prompt a thorough evaluation, and skull fracture is no exception (95,96).

Radiologic Appearance.—Radiography of the skull is preferred over CT, because fractures parallel or nearly parallel to the section orientation are missed at CT (97). Four views of the skull (anteroposterior, both lateral views, and a Towne view) constitute the standard skull radiographic series. Two views (anteroposterior and lateral) are recommended as part of the skeletal radiographic survey, with additional views taken as necessary, especially if head trauma is suspected (98). Fractures appear as linear or branching lucent areas with sharp margins. Diastasis (separation of 3 mm or more) may also be observed. Scintigraphy is not recommended, since it has been shown to be relatively insensitive for the detection of skull fracture (Fig 18) (30).

Interhemispheric Extraaxial Hemorrhage

Subdural hemorrhage (SDH) and subarachnoid hemorrhage (SAH) are common abusive injuries. Epidural hematoma is much more often accidental than inflicted and may result from relatively short falls. Thus, epidural hematoma is not a specific indicator of inflicted injury. In three studies of 177 children with intracranial injury, only four cases of inflicted epidural hematoma were discovered (77,84,99). SDH and SAH are much more common injuries in the abused child. In a series of 287 children aged 1 week to 6.5 years old with head injuries, SDH was found in 46% and SAH was discovered in 31% of children with NAHI (compared with 10% and 8%, respectively, in children with accidental head injury) (100). Another study of 99 children with head trauma who were less than 2 years old determined that SDH occurred in 69% of children with NAHI, compared with 7% in those with accidental head injury (101). The prevalence of SAH varies considerably with the report; it is almost invariably documented at autopsy in children who die of NAHI (77). Neither SDH nor SAH are specific for abuse, however, since SDH may result from birth. In two recent reports of 35 asymptomatic term infants who underwent brain magnetic resonance (MR) imaging within a few days of birth, 16 infants (all vaginally delivered) had evidence of parafalcine or tentorial SDH (102,103).

SAH results from shearing of bridging veins as they exit the brain, cross the extraaxial spaces and membranes, and continue to the venous sinuses. SAH may also occur from direct contact forces (a blow to the head), which cause tearing of vessels. Blood accumulates subjacent to the arachnoid membrane, in the subarachnoid space, which normally contains only cerebrospinal fluid. SAH fills the fissures and sulci in the region of hemorrhage (104). SAH is best demonstrated with CT; the use of MR imaging for detection of acute SAH remains controversial, although the addition of specialized pulse sequences may increase the detection rate (105).

Probably the most common location of inflicted SAH and SDH diagnosed radiologically is a layer of hyperattenuating material adjacent to the falx; bleeding in this site represents an interhemispheric extraaxial hemorrhage (Fig 20) (94). In this location, it is often difficult, radiologically, to distinguish SAH from SDH, and SDH and SAH may coexist here (86,106,107). Interhemispheric extraaxial hemorrhage is the result of shearing of bridging veins as they travel to the sagittal venous sinuses; it is often associated with convexity extraaxial hemorrhage that may be difficult to discern at CT as the convexity transitions

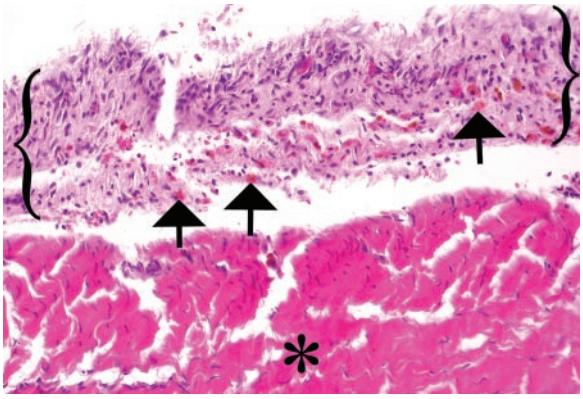

Figure 21. Dura from an abused 3-month-old infant who sustained a head injury. Low-power photomicrograph (original magnification, ×20; hematoxylin-eosin stain) shows that the subdural membrane (within the brackets) is composed of organizing granulation tissue, indicating prior hemorrhage. The normal dura (*) is at the bottom of the image. Hemosiderin-filled macrophages (arrows) are plentiful.

to the skull (104). In one experienced pediatric neuroradiologist's opinion, interhemispheric SDH has the highest specificity for abuse of any intracranial injury, although it may be caused by serious accidental trauma such as motor vehicle accidents (94). Its significance for abuse rests with the causative mechanism: to-and-fro head motion with shearing of midline veins (82,108).

SDH, like SAH, usually results from shearing of bridging vessels when they are subjected to significant forces (109,110). A brief review of the meningeal coverings of the brain may help one to better understand the predilection of the subdural space for hemorrhage. The outermost layer of dura mater is adherent to the inner table of the skull and is in fact the inner periosteum (also known as the periosteal dura). Bleeding between the periosteal dura and the skull is an epidural hematoma. Contiguous with, and immediately subjacent to, the periosteal dura is the inner, or meningeal, dura. These two dural layers are intimately apposed everywhere except the venous sinuses, where they separate to form the sinuses. Just deep to the meningeal dura (and contiguous with it) is the arachnoid membrane. There is normally no subdural space between the meningeal dura and the arachnoid membrane, and nothing naturally exists here (111,112). However, when vessels traversing the extraaxial space bleed, they may do so into this potential space, resulting in a SDH. Beneath the arachnoid membrane is the subarachnoid space, which contains vessels and cerebrospinal fluid. Hemorrhage into this space is called SAH (113). Finally, the brain is tightly covered by pia mater, which delimits the inner extent of the subarachnoid space. Bleeding deep to the pial surface is considered intraaxial in location.

What is unusual about SDH is the frequency with which hemorrhage occurs in the potential space. One possible explanation is that cortical bridging veins, as they pass through this space, have very thin areas in the vessel walls, which are believed to be prone to rupture when stressed (114). Another factor may be that the innermost portion of the meningeal dura (the so-called dural border cell layer, immediately adjacent to the arachnoid membrane) is itself weak, lacking much of the collagen and intracellular junctions found in the arachnoid membrane (115). Thus, a cleavage plane may form within the dural border cell layer from mechanical separation. Hemorrhage into this cleavage plane results in a SDH (116).

Typically, the small volume of SDH seen in most cases of childhood NAHI is not, in and of itself, responsible for neurologic compromise (117). In infants and small children, the SDH serves as a marker for rotational brain movement (acceleration and deceleration). Larger SDHs, although rare, may be associated with effects typical of a space-occupying lesion (118). This is in contrast to the larger SDHs often seen in adults—particularly frequent in alcoholics and the elderly—for whom the size and mass effect of the hemorrhage warrant the more appropriate designation of "hematoma." In this adult population, these space-occupying hematomas readily account for neurologic effects through a variety of mechanisms not yet well understood, including local vascular compromise and remote mechanical forces on structures such as the thalamus and corpus striatum (119).

Pathologic Characteristics.—At gross examination, an acute SDH appears as a clot deep to, and easily separable from, the pristine dura mater. A fresh SDH shows no reactive changes histologically. Subsequent changes develop between the clot and dura, with the associated meninges serving as the source of connective tissue elements and migrating leukocytes. The earliest changes in subdural organization include leukocytic infiltration (initially granulocytes, then macrophages), followed by hemosiderin deposits with neovascularization and then collagen production in the clot. Reactive changes are variable and do overlap. The earliest changes probably begin within 1–2 days after injury; the others, subsequently.

The connective tissue eventually organizes into a membrane. Studies of adults with atrophy and chronic SDH indicate that an outer membrane forms within 24 hours; it is completely formed within a week (Fig 21). A thinner inner membrane forms gradually over the first 3 weeks.

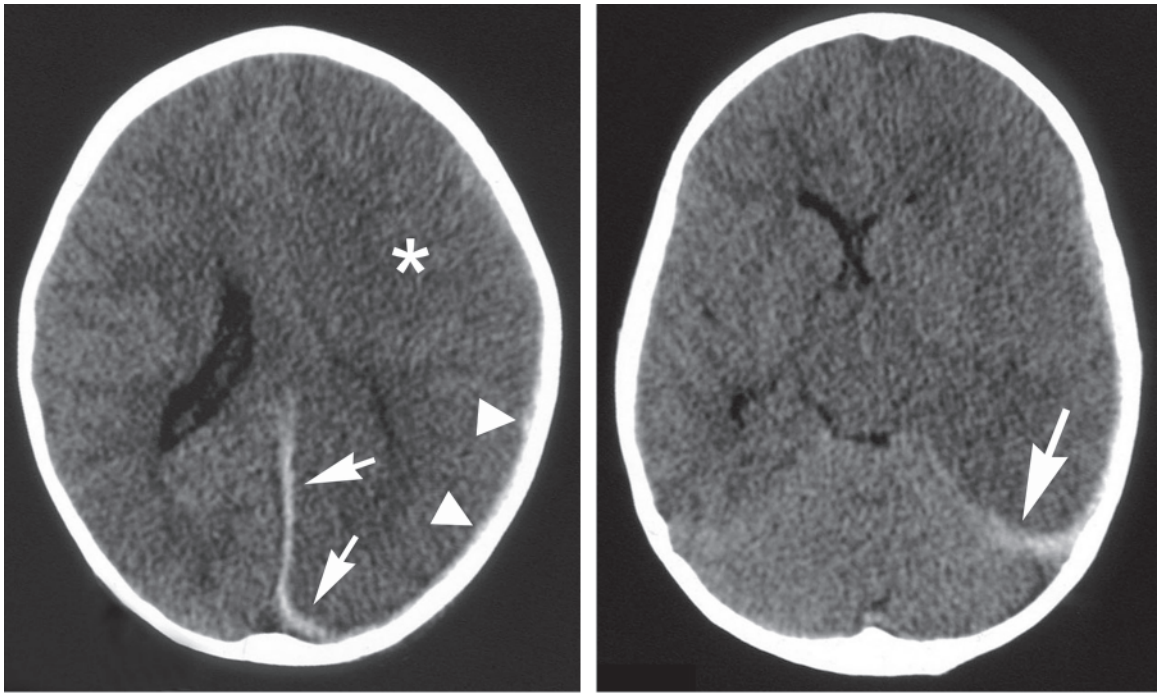

a. b.

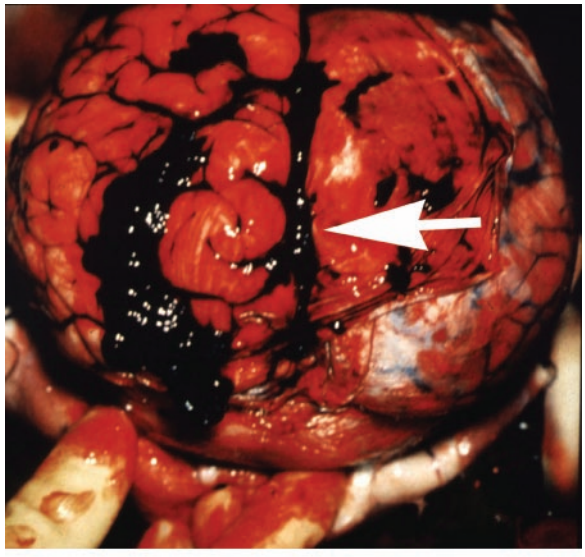

c.

Figure 22. Extraaxial hemorrhage and edema in a fatally abused 3-year-old boy. **(a)** Axial unenhanced CT scan, obtained through the cerebral hemispheres at the level of the lateral ventricular atria, reveals diffuse left hemispheric edema, manifest as parenchymal low attenuation (*), sulcal effacement, and left lateral ventricular effacement. There is high-attenuation blood in the posterior interhemispheric fissure, extending to the left of the superior sagittal sinus (arrows) and along the left convexity (arrowheads). **(b)** Axial CT scan obtained at the level of the mesencephalon reveals high-attenuation extraaxial blood along the left tentorium cerebelli (arrow) and left hemispheric edema. **(c)** Autopsy photograph of the brain (vertex view, with the skull removed, patient's left on the left) reveals blood in the interhemispheric fissure (arrow), extending as thin layers of SAH and SDH over both convexities, left greater than right.

Thus, within several weeks, the SDH is encapsulated by fibrous inner and outer membranes, which are fused at the periphery of the SDH, resulting in a chronic SDH (116,120). Within these membranes are numerous, proliferating capillaries, some of which are fragile and lack complete basement membranes; this suggests that they may be prone to hemorrhage, and studies in adults have shown that these vessels do in fact bleed into preexisting chronic SDH (114,121–123). Other studies have suggested that defective coagulation in adult chronic SDH may interfere with hemostasis if these fragile vessels bleed (124–126). The classically described chronic SDH, which is typically seen in patients with brain atrophy (the elderly or alcoholic patient) is rarely, if ever, discovered in children (118).

For a number of reasons, relating radiologic and histologic changes within subdural hematomas may be difficult. Histologic "dating" of subdural hematomas is imprecise, and caution must

Figure 23. Mixed attenuation SDH and cerebral edema in an abused 8-month-old infant. Axial unenhanced CT scan obtained at the level of the lateral ventricles depicts a mixed attenuation SDH along the left convexity (arrows). There is also a thin interhemispheric extraaxial hemorrhage (arrowheads) and left cerebral edema.

be emphasized in such interpretations, since the published database for hematoma aging is rather old and based on an adult population (127). In children who survive initial inflicted head injury but later succumb to complications, there may be considerable time elapsed between initial radiologic examination and postmortem examination. Finally, as with many types of abusive injuries, there are few (if any) known standards against which to compare. Corroborated or witnessed accidental injuries are uncommon, and if initially survived, are less likely to be fatal than inflicted injuries. In abusive injuries, the actual timing of the injury is often suspect, as histories are misleading and at odds with the physical and radiologic findings.

Radiologic Appearance.—SDH appears as a crescentic convexity or interhemispheric (parafalcine) collection (Fig 22). The appearance of SDH at CT is classically described as high attenuation when the hemorrhage is acute, becoming isoattenuating relative to brain, and finally hypoattenuating as the SDH ages over days to weeks (128). However, the exact time frames of these changes are not well established and may vary considerably from patient to patient (129,130). Layering may also occur, with a more cellular, hemoglobin-rich dependent area with an upper layer of fluid with low hemoglobin content (131). Membrane(s) may be visible with contrast material enhancement, suggesting a SDH that is a week or more old (132,133). Active bleeding may cause a mixed attenuation in an acute SDH, which may be mistaken for a subacute SDH or multiple SDHs (Fig 23) (94,134,135). A recent study of SDH resulting from known motor vehicle accidents in 18 children less than 2 years old was remarkable in that three of the SDHs were in part hypoattenuating on the day of trauma. It is theorized that disruption of the arachnoid membrane during trauma allows cerebrospinal fluid flow into the SDH, diluting the hemorrhage and reducing its attenuation at CT (136).

MR imaging shows even small SDHs particularly well, given its multiplanar imaging and ability to exploit tissue differences with different parameters (Fig 24). MR imaging is superior to CT for differentiation between hypoattenuating SDH and cerebrospinal fluid and for detection of small extraaxial fluid collections (79,105). Acute SDH (1–3 days after injury) appears isointense to hypointense on T1-weighted images and hypointense on T2-weighted images. In the early subacute time frame (3–7 days), blood is hyperintense on T1-weighted images and becomes

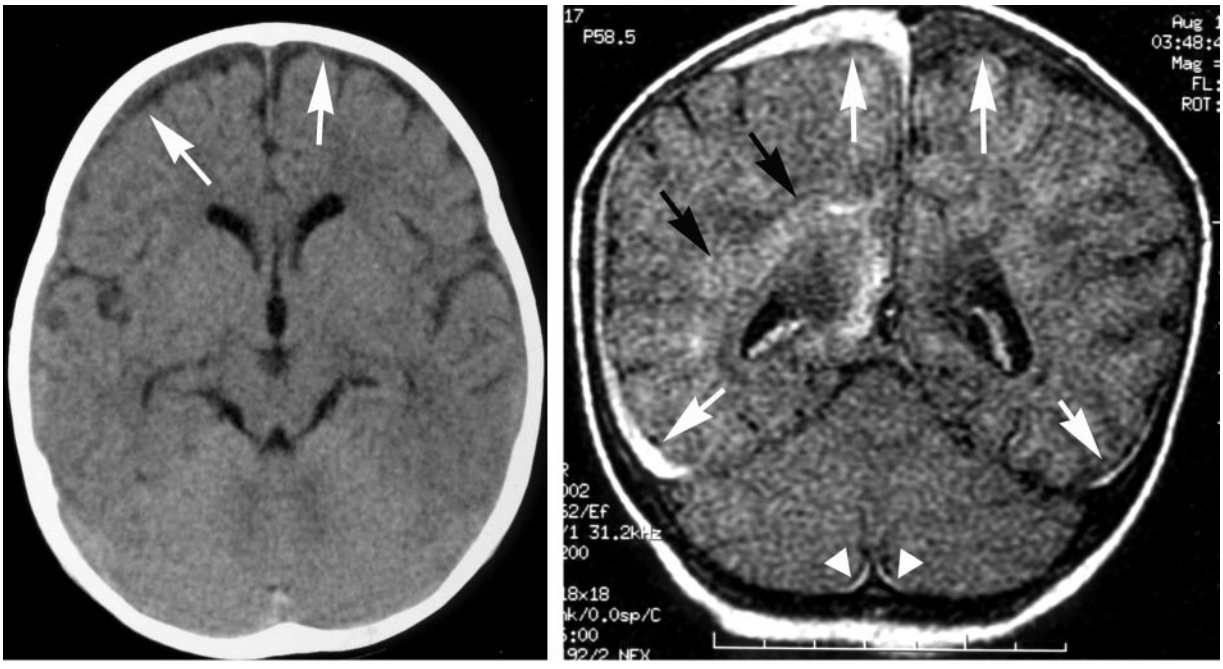

a. b.

Figure 24. Multiple SDHs in a head-injured 4-month-old boy. **(a)** Axial unenhanced CT scan of the brain obtained at the level of the frontal horns reveals subtle increased attenuation of the extraaxial fluid over both convexities (arrows). **(b)** Coronal MR image (repetition time msec/echo time msec = 9,002/162; inversion time, 2,200 msec) of the brain taken 4 days later reveals intermediate- to high-signal-intensity SDH over the left convexity and high-signal-intensity SDH over the right (white arrows). Both of these fluid collections are brighter than the intraventricular cerebrospinal fluid. Small, high-signal-intensity SDHs are visible in the posterior fossa (arrowheads), and there is high signal intensity in the right hemispheric parenchyma, indicating edema (black arrows).

hypointense on T2-weighted images. Late subacute blood (8–14 days) appears hyperintense on both T1- and T2-weighted images. Finally, as the blood products age, they transition from being hyperintense on both T1- and T2-weighted images to being isointense to hypointense on T1-weighted images and hypointense on T2-weighted images (137). These are general guidelines, however, and as with the appearance of SDH at CT, injury dating should be approached cautiously. Contrast material enhancement of SDH and meninges has been observed in an abused infant, increasing lesional conspicuity (138).

Recently, ultrasonography (US) has been investigated as a means to visualize the extraaxial spaces and brain in infants. It is very useful for discrimination of symmetric, diffuse enlargement of the subarachnoid spaces (also known as benign external hydrocephalus of infancy) from low-attenuation SDH, which may be difficult at CT. At US, the subarachnoid space is characterized by multiple crossing vessels (cortical veins) in anechoic fluid, lack of any linear echogenicities paralleling the cortex that would suggest membranes, and lack of mass effect. An abnormal subdural collection (which may be due to meningitis or SDH) at US typically appears as variable echogenicity fluid with few or no cortical veins (Fig 25). A thickened inner membrane may be seen; this finding is regarded as a useful sign of an abnormal

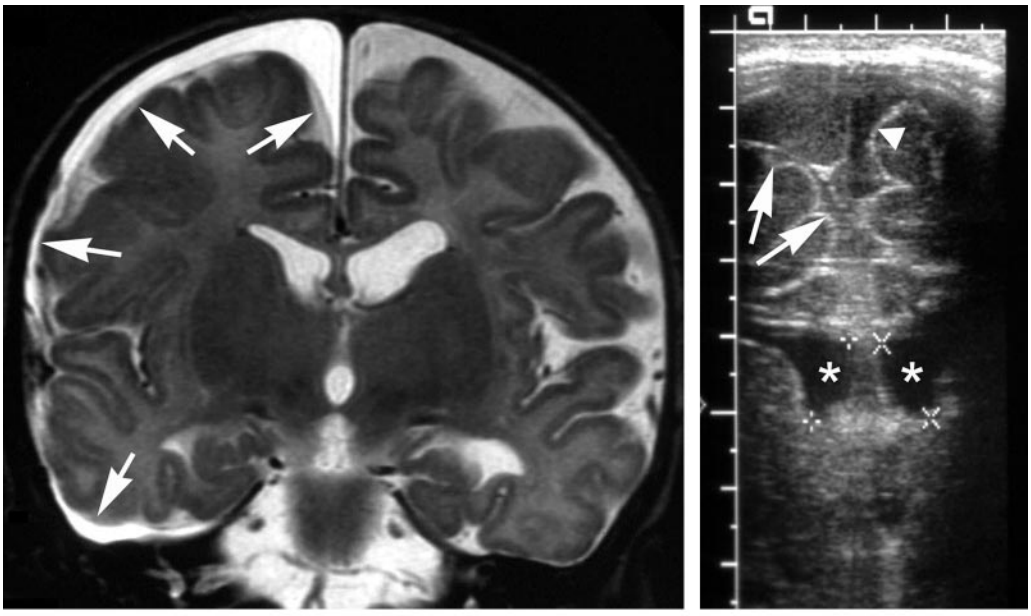

a. b.

Figure 25. SDH in an abused 3-month-old girl. **(a)** Coronal T2-weighted (2,000/105) MR image reveals a high-signal-intensity SDH over the right convexity, extending into the interhemispheric (parafalcine) region (arrows). **(b)** Magnified coronal sonogram of the brain vertex obtained with a linear 7.5-MHz transducer shows the echogenic fluid over the right convexity and in the parafalcine subdural space (arrows). The lateral ventricles are filled with anechoic cerebrospinal fluid (*). Normal, prominent subarachnoid cerebrospinal fluid is visible over the left convexity (arrowhead).

subdural space. Limitations of US include its relatively poor depiction of the posterior fossa and far convexities and its inability to demonstrate the nature of abnormal fluid collections (SDH or effusion associated with meningitis) (139). Its greatest utility at the present time is as a convenient method of following an abnormality previously documented at CT or MR imaging.

Rebleeding.—It is well established that the outer membrane of SDH may bleed into the existing hematoma cavity in chronic SDH in adults. This fact has led to speculation that preexisting SDH could undergo spontaneous, massive rehemorrhage (with little or no precipitating trauma), resulting in severe neurologic compromise and even death. However, there is nothing in the literature to support this contention, and no such case has ever been reported in an infant or child, even under verifiably accidental circumstances. Thus, a massive, symptomatic rehemorrhage into a preexisting SDH remains a speculative, unproved theory (93,118,140–142).

Brain Parenchymal Injury

The brain itself may be intentionally injured in virtually every way imaginable, particularly when the head is subjected to excessive rotational movement resulting in acceleration-deceleration (also known as shearing or shear-type) forces. The three most commonly observed patterns of brain parenchymal injury are shear injury, contusion, and edema.

Shear Injury.—The brain is relatively intolerant of shearing forces and deforms readily in response to shear stress (143,144). The brain parenchyma shears at the gray-white junction, where the differing densities of the tissue make the brain particularly susceptible to shearing forces. Shear injury is detectable on a microscopic and sometimes a macroscopic level. Shear injury is often referred to as *axonal injury*, which may be diffuse or focal. Macroscopic shear injury has been variously called *white matter tear* and *contusion tear*, which is a rare, although well-described, manifestation

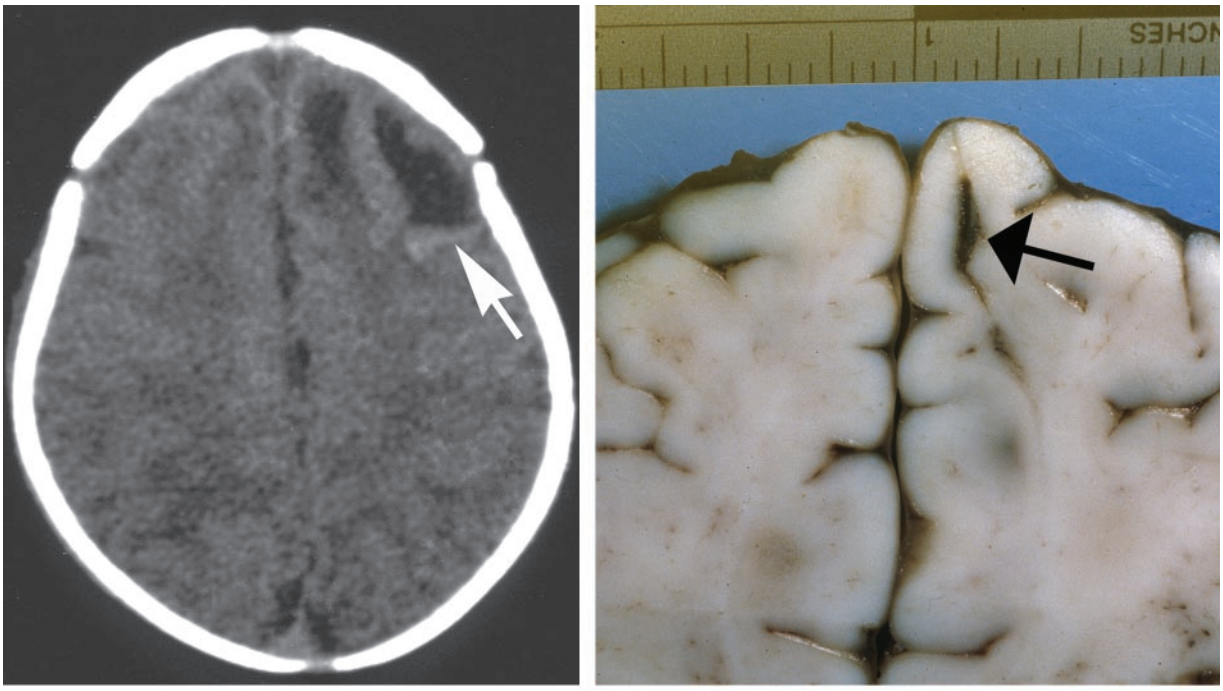

a. b.

Figure 26. White matter tear in a fatally abused 7-week-old boy. **(a)** Axial CT scan of the brain shows a fluid-filled cavity in the left frontal white matter, with blood layering posteriorly (arrow). **(b)** Autopsy photograph of the fixed and sectioned brain shows the collapsed tear (arrow) in the left frontal lobe.

of rotational head injury (Fig 26) (118). Typically, when this rare lesion is found, it is in infants younger than 5 months (145–147).

The histologic hallmark of axonal injury is the spheroid or retraction ball (Fig 27) (148). Briefly, shear stress imparted to the brain initiates a series of events, resulting in disruption of axonal cytoplasmic flow. There is focal accumulation of cytoplasm (retraction balls or spheroids) along portions of the axon, which is best demonstrated with beta amyloid precursor protein (βAPP). This injury occurs in infants and young children most commonly in the deep white matter, corpus callosum, and midbrain (149).

The demonstration of βAPP within these tissues can help delineate axonal injury. βAPP is a neuronal protein that accumulates in the injured axon and may function as a protectant (150–152). A monoclonal antibody directed against an antigen of βAPP, when used in the form of a special stain, reveals injured axons within tissue sections with greater sensitivity than standard staining techniques. This staining method is not absolutely specific for trauma, however, since it identifies ischemically injured axons as well (152). Pathologists rely on different staining patterns at the histologic level to distinguish between these two conditions. Traumatic patterns include discrete retraction ball labeling in corticospinal tracts and the deep white matter. Hypoxic changes include a relatively diffusely stained background of hypoxic-ischemic tissue with perivascular absence of staining, as well as delineation of infarcts and vascular boundary areas (149,153). Such distinctions are not always possible in actual practice.

One advance already obtained with this technology is the demonstration of axonal injury within the cervical spinal cord and nerve roots (149,153,154). At present, it is not known whether this finding is caused by a concentration of mechanical forces at the neck region or by preservation of perfusion that allows βAPP to accumulate. In either event, these findings correlate with the apnea commonly encountered clinically (155).

Global hypoxic changes are a common, and at times disastrous, consequence of abusive head trauma. Injury and swelling result in severe damage due to inadequate perfusion. The so-called

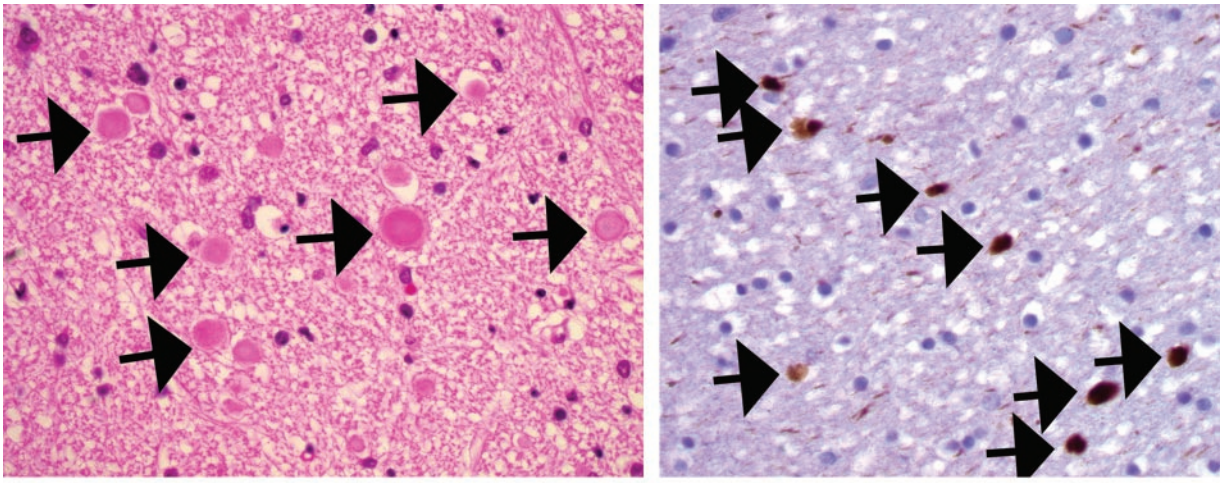

a. b.

Figure 27. Axonal spheroids in shear-type NAHI. **(a)** High-power photomicrograph (original magnification ×400; hematoxylin-eosin stain) of the medullary corticospinal tract from a 3-month-old infant reveals axonal injury as axonal enlargements or spheroids (arrows). **(b)** High-power photomicrograph (original magnification, ×400; βAPP with hematoxylin stain) of a pontine corticospinal tract from a 2-year-old child clearly shows axonal spheroids (arrows).

respirator brain, or more preferably *nonperfused brain,* is diffusely edematous, friable, and commonly herniated. The histologic specimen may show red discoloration of neurons (indicating necrosis) and edema, whereas additional changes are hampered by diminished perfusion. This includes diminished βAPP accumulation, since βAPP accumulation relies on active transport. For these reasons, histologic studies are most useful in the early postinjury period (156). With longer postinjury intervals, one must rely on other features of injury such as SDH and eye findings.

At CT, axonal injury may be occult, especially because it is uncommonly hemorrhagic in infants. High-attenuation petechiae may be evident at CT if the axonal injury is hemorrhagic. There is often a background of focal or diffuse edema (low attenuation). MR imaging is preferred for the detection of axonal injury. Nonhemorrhagic axonal injury is hyperintense on T2-weighted images; when hemorrhagic, axonal injury is typically hyperintense on T1-weighted images and hypointense on T2-weighted images. Fluid attenuating inversion-recovery (FLAIR) MR imaging may show axonal injury to particular advantage as hyperintense areas (157).

Gross white matter tears are detectable with CT, MR imaging, and US (which was shown to be superior to CT for detection of white matter tears in one study). At CT, they appear as well-defined, low-attenuation areas in the subcortical white matter (often frontal or parietal in location), occasionally with blood layering dependently (Fig 26). At MR imaging, they follow cerebrospinal fluid signal intensity (158). At US, they appear as anechoic or hypoechoic fluid collections within the brain substance, often with an echogenic rim (159).

Contusion.—Cerebral contusion is a focal hemorrhage within the brain parenchyma (usually involving the cortex) that results from direct contact forces. Such injuries are distinctly rare in infants. They are typically small and thus difficult to demonstrate at CT, unless they are grossly hemorrhagic (Fig 28) (160). Commonly contused areas are the frontal lobes, temporal lobes, and parafalcine cortex. MR imaging provides superior lesional conspicuity, especially with the use of gradient-echo pulse sequences to detect small amounts of hemoglobin (79,105). Contusions may evolve into focal areas of encephalomalacia with cystic cavities (161,162).

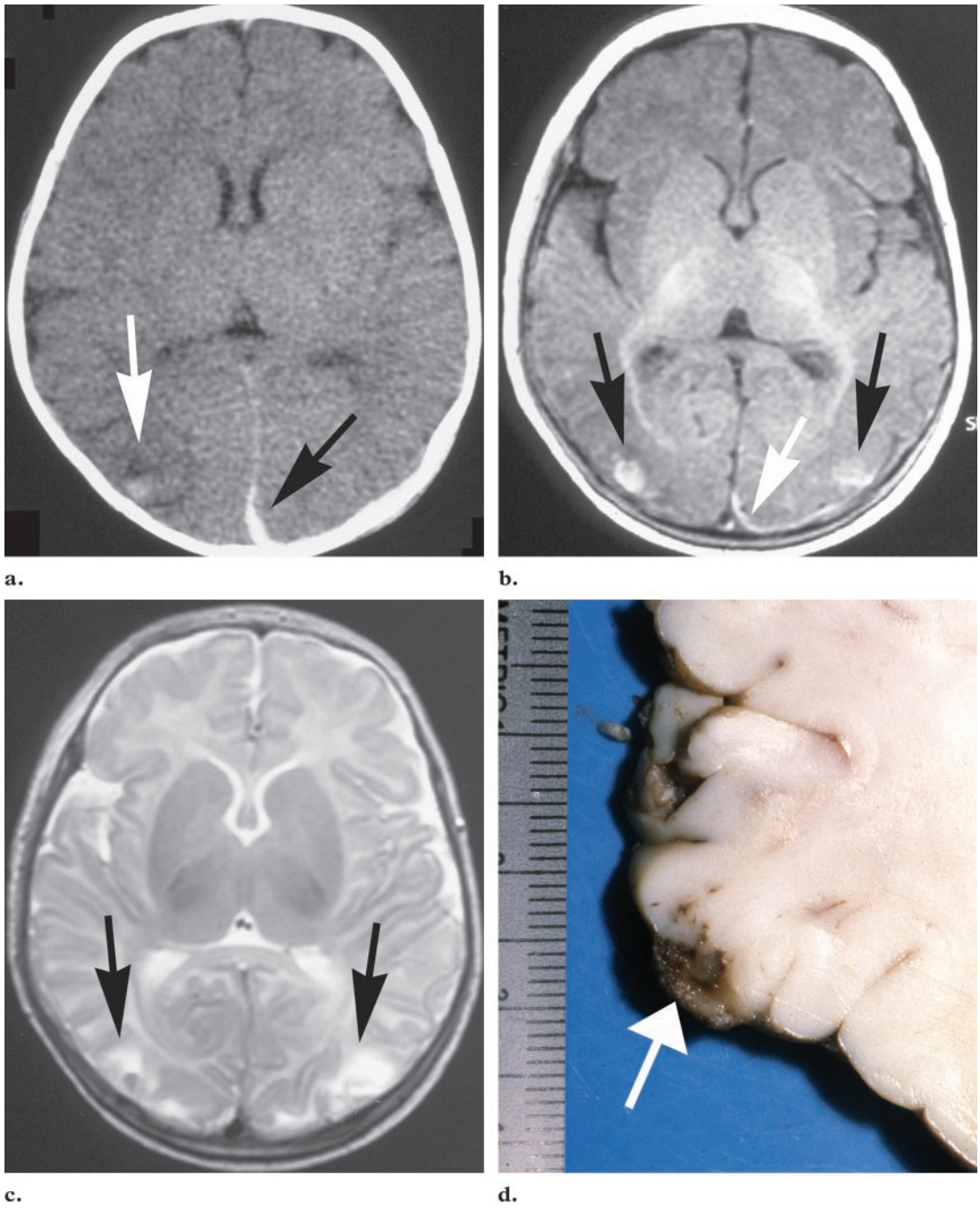

Figure 28. Occipital contusion in a fatally abused 2-month-old girl. **(a)** Axial unenhanced CT scan shows interhemispheric hemorrhage (black arrow) and a small area of high attenuation in the right occipital lobe (white arrow). **(b)** Axial T1-weighted (600/15) MR image shows areas of high signal intensity in both occipital lobes (black arrows), as well as interhemispheric and left convexity extraaxial hemorrhage (white arrow). **(c)** T2-weighted (2,200/115) MR image reveals these areas of parenchymal contusion (arrows) as slightly larger than those seen with T1-weighted imaging and of high signal intensity, compatible with hemorrhage and edema. **(d)** Autopsy photograph of the fixed brain shows the hemorrhagic nature (brown pigmentation) of the right occipital contusion (arrow). Scale is in centimeters.

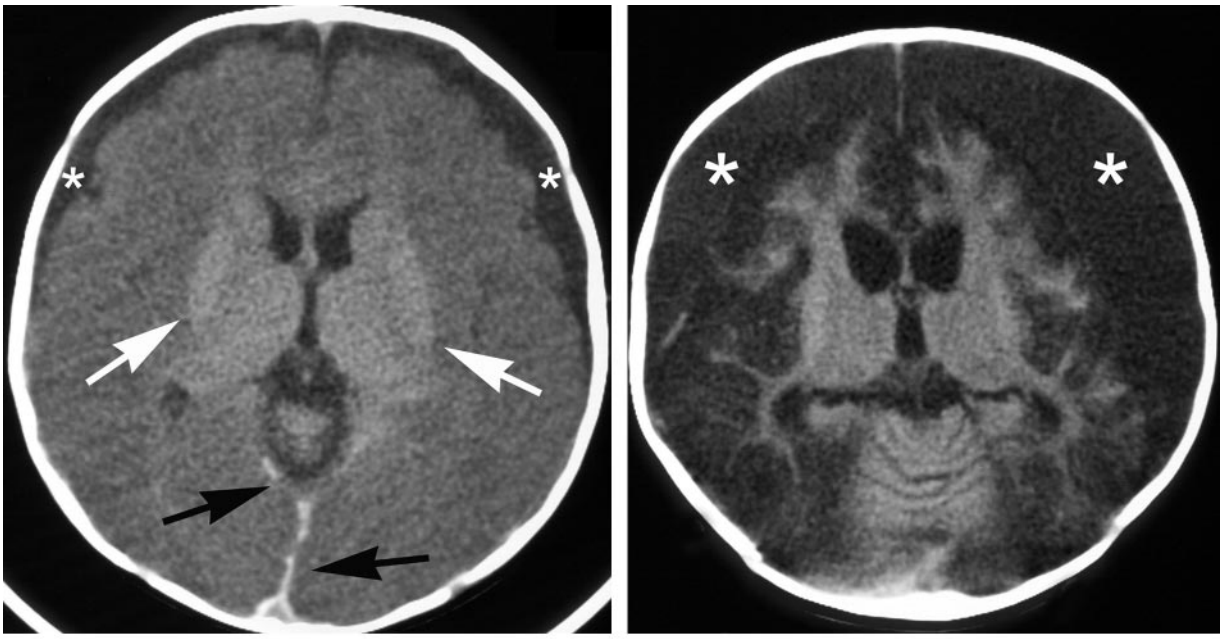

a. b.

Figure 29. Reversal sign in a 3-month-old boy with abusive head injury. **(a)** Axial unenhanced CT scan depicts low attenuation, with loss of gray-white matter differentiation, throughout both hemispheres. There is relative high attenuation of the basal ganglia and thalami (white arrows). Also seen is low-attenuation SDH bilaterally (*) and interhemispheric and tentorial hemorrhage (black arrows). **(b)** Axial unenhanced CT scan obtained 18 days later reveals generalized cerebral atrophy and large bilateral low-attenuation SDH (*), likely enlarged by the rapid atrophy with resultant tension on the bridging veins.

Cerebral Edema.— Edema, focal or diffuse, is a common feature of NAHI. It may be a manifestation of primary injury or the consequence of hypoxia, and it may be seen in a variety of other settings including strangulation, suffocation, posttraumatic apnea, and other causes. Thus, edema is a marker of brain injury and not a specific finding (104). Edema may also be caused by impedance of venous return from chest compression (162). As the brain swells, compression of vessels and elevated intracranial pressure may further compromise the cerebral vascular supply, resulting in more injury, edema, and possibly herniation. Posttraumatic apnea has been suggested as a cause of some of the edema noted in abused infants (155). This theory is supported by several discoveries, one being the presence of craniocervical junction and cervical spinal cord injuries in victims of shaking, which may lead to apnea or hypoventilation, as already discussed (149,163–165). The other is the visualization of normal vascularity on a background of restricted free water diffusion (see the following discussion on MR imaging) seen in early posttraumatic diffusion-weighted MR imaging of abused infants (166,167).

At CT, edema manifests as focal or diffuse low attenuation, associated with loss of distinction between gray and white matter and, if the edema is of sufficient magnitude, evidence of mass effect (sulcal effacement, herniation) (86). Global edema may contrast sharply with the normal hyperattenuating vascular structures of the brain (eg, venous sinuses, circle of Willis) and may simulate the appearance of SAH or parafalcine hemorrhage. Profound, diffuse edema in infants has an unusual tendency to maintain normal attenuation of the basal ganglia, thalami, brain stem, and cerebellum (Fig 29). This appearance has been called the *reversal sign* by Han and colleagues (168); it is also referred to as the *bright cerebellum sign* (169). The reasons for the normal attenuation of these structures is not well understood.

At MR imaging, edema appears as hyperintense cortex on T2-weighted images (105). The white matter edema may be difficult to appreciate, given that the very immature, unmyelinated brain has a high water content. Recently, diffusion-weighted imaging has been used to detect early cytotoxic edema in NAHI when findings from MR imaging performed with other pulse sequences appear normal. Areas of restricted water diffusion appear bright on diffusion-weighted images (Fig 30). Not only does diffusion-weighted imaging depict changes of ischemia

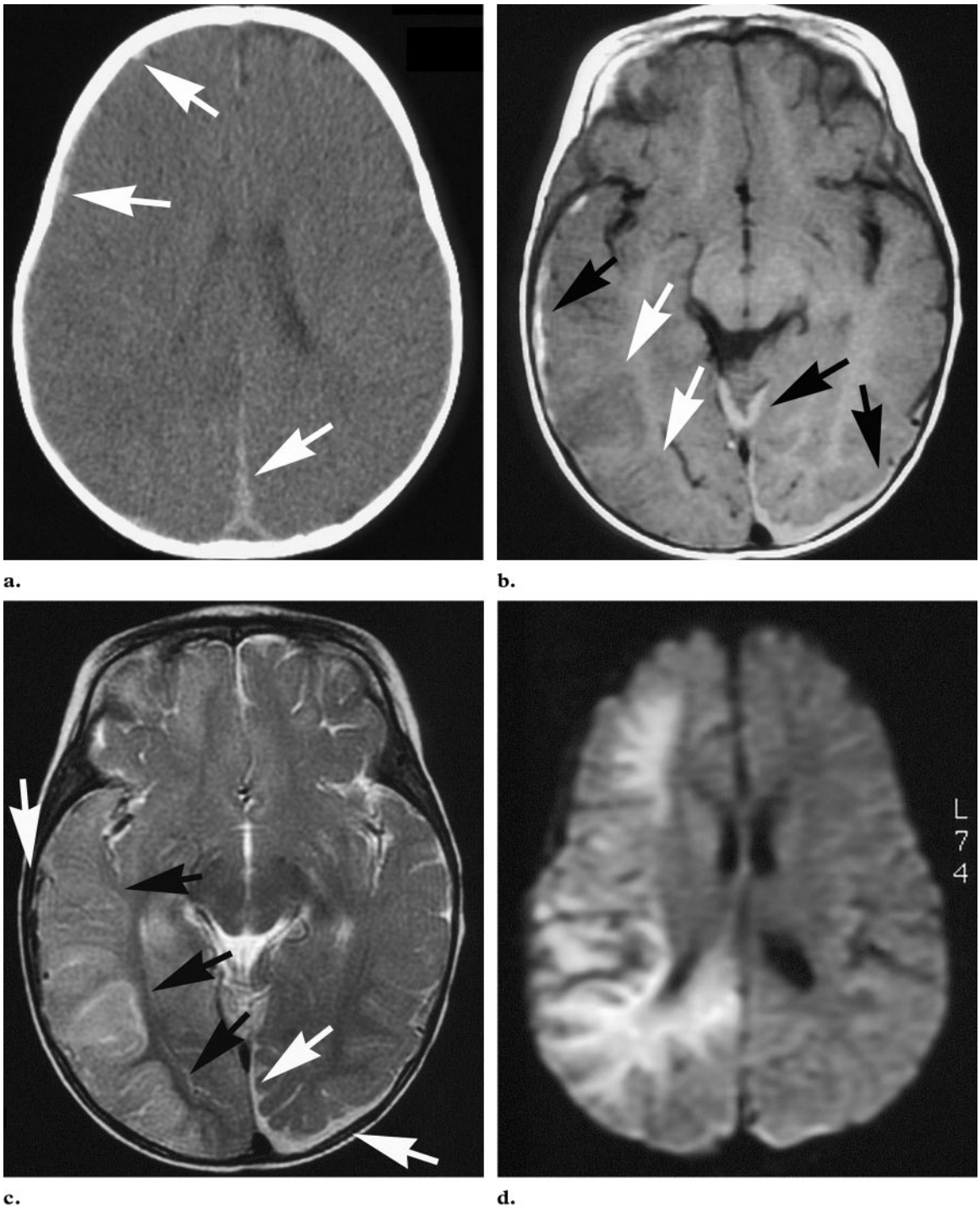

Figure 30. Diffusion-weighted MR imaging in a 9-month-old girl with abusive head injury. **(a)** Axial unenhanced CT scan obtained on the day the child presented with seizure shows right hemispheric sulcal effacement, loss of gray-white matter differentiation, and a thin rim of extraaxial blood along the right convexity and in the interhemispheric region (arrows). **(b)** Axial T1-weighted (516/12) MR image obtained the same day as the CT scan reveals low signal intensity of the right temporal and occipital lobes (white arrows) and high-signal-intensity SDH over the convexities, in the posterior interhemispheric region, and in the tentorial incisura (black arrows). **(c)** Axial T2-weighted (3,200/99) MR image at the same level and from the same day reveals increased signal intensity of the right temporal and occipital lobes (black arrows) and high-signal-intensity SDH over the convexities bilaterally (white arrows). **(d)** Diffusion-weighted (9,999/96) MR image obtained the same day reveals marked elevated signal intensity throughout the right hemisphere compatible with restricted free water diffusion.

very early, it also demonstrates more and larger areas of involvement in NAHI compared with MR imaging performed with other sequences (166,167). This finding is seen in 10 minutes to 2 hours in experimental animals; in adult humans, it has been seen as early as several hours after onset of symptoms (170). The abnormality seen at diffusion-weighted imaging normalizes in approximately 10–14 days, although the normal appearance of the tissue should not be taken as evidence that the injury has resolved (171).

Biomechanics of Head Trauma

Although abuse can produce any head injury, including scalp contusion, subgaleal bleeding, skull fracture, epidural hematoma, and cerebral contusion, attention has largely been focused on the SDH and brain injury characteristic of the "shaken baby syndrome." Experimental work done with primates in the 1960s established rotational acceleration as the leading biomechanical explanation for these injuries (172). Caffey cited this work when developing his theories on infant shaking and abusive injury (173). Ommaya et al (174), the principle investigators in the primate experiments, have objected to Caffey's hypothesis, stating that shaking is unlikely to produce adequate rotational acceleration to be injurious (174). Duhaime et al (160) demonstrated this by shaking instrumented doll models in the 1980s. Although these authors have raised questions about the injuriousness of shaking-induced rotation, rotational acceleration has remained the leading biomechanical explanation for these injuries.

Under the rotational acceleration theory, sudden changes in rotational motion produce relative movement between the brain and the skull and shearing strains within the brain (175). This motion is analogous to giving a sharp twist to a cup of coffee. The cup twists around the coffee, and the outer rim of coffee spins at a different rate than the center. When the brain is subjected to rotational acceleration (such as when an infant is shaken), bridging veins that cross from the dural sinuses to the brain are stretched, tear, and bleed into the subdural and subarachnoid spaces. Axons that run between superficial and deeper areas of the brain are also stretched, resulting in axonal injury. The same concept has been used to explain retinal hemorrhages (176,177). During sudden rotation of the eye, the globe moves relative to a lagging vitreous. This disparity in movement produces traction on the retina, leading to retinal bleeding, retinal folds, and retinoschesis (a tearing apart of the layers of the retina) (177).

The principal biomechanical controversy in abusive head trauma questions the circumstances under which injurious rotational acceleration occur. As noted, experiments with instrumented dolls failed to produce the quantities of acceleration found to be injurious in primates (160). Although recent experiments with new biofidelic (ie, simulating normal) infant models have suggested that the forces occurring during shaking may be greater than earlier estimates, levels associated with diffuse axonal injury were still not reached. These results have led to biomechanical arguments that shaking alone cannot cause shaken baby syndrome and that impact-associated acceleration is a necessary factor in causing these injuries. A major weakness in any biomechanical analysis of intracranial injury of infants is the lack of data on the rotational tolerance of the immature brain and the effect of repeated acceleration, similar to shaking, on the brain and bridging vessels. Until these issues are resolved, the biomechanical answer to the shaking versus impact controversy will not be forthcoming.

Epidemiologic studies have found that many babies with shaken baby syndrome lack any external evidence of impact (178,179). In addition, a well-documented case of a repeatedly and violently shaken adult with no history or pathologic evidence of impact demonstrated thin convexity SDH and malignant cerebral edema, similar to that found in infants with shaken baby syndrome (180). Also of note, retinal hemorrhages are found much less frequently in infants with intracranial injuries from motor vehicle collision and other accidental causes (2% of cases) than in infants with abusive injuries (28%) or the classic shaken baby syndrome (80%–90%) (77,176,181–184). The clinical outcome of infants with shaken baby syndrome is generally worse than that of infants with intracranial injuries from motor vehicle collision (182). It is clear that something is different about these shaken babies, and many believe that this difference is explained by shaking.

Recently, the rotational acceleration hypothesis itself has been questioned. Physicians have often wondered why the violent shaking they hypothesized did not result in cervical injury (174). Cervical injury is infrequently found in living patients with shaken baby syndrome, even with modern imaging techniques (185). Injuries to the craniocervical junction, cervical spinal cord system, and cervical tissues have been described at autopsy,

however (149,163,185). Pathologic studies, looking for evidence of both diffuse axonal injury and cervical injury, have supported the supposition that brain injury is actually from hypoxic-ischemic causes, due to cardiorespiratory changes from mechanical injury to pontine, medullary, and cervical nuclei (154). According to this theory, flexion and hyperextension of the neck during shaking may cause brain stem injury and attendant difficulties with breathing and circulation, resulting in acute and chronic injury to the brain. Unfortunately, this theory fails to address the additional findings of SDH and retinal hemorrhage.

The term *shaken baby syndrome* has become entrenched and comes all too easily after 30 years of use. Although shaking is likely to be an important factor in abusive head injury, contact injuries and injury during the acceleration that accompanies impact are often found but are not strictly consistent with the diagnosis of shaken baby syndrome. Physicians who use the term shaken baby syndrome must understand both the foundation and the controversies surrounding the shaking hypothesis. Additional injuries not explained within the shaking hypothesis must be explained by additional or alternate diagnoses. It is important that abusive injury be recognized as abuse independent of the biomechanical controversies.

Visceral Injury

Visceral injury is estimated to account for just 2%–4% of all abusive injuries, although it is responsible for 12% of all abuse-related deaths (24,186,187). These reports are from older literature, however, before the widespread use of CT, and therefore likely underestimate the true prevalence of visceral injury. Clinically apparent visceral injury is associated with a 45%–53% mortality rate (188–190). Delay in seeking care (itself a form of child abuse) contributes, often substantially, to the high mortality, as often these children are not seen until they have developed peritonitis, sepsis, or vascular collapse (191). Thus, abdominal injury is not the most common form of abuse-related injury, but it is highly lethal. Visceral injury has been reported in abused children of all ages.

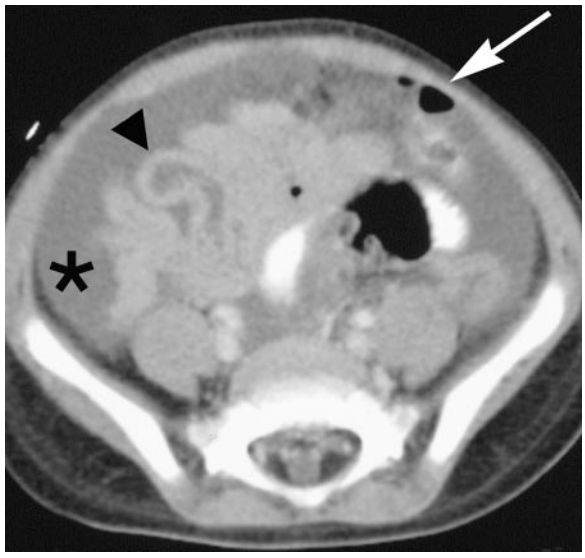

Figure 31. Bowel injury and perforation in an 18-month-old boy who was beaten. Axial CT scan through the midabdomen, obtained after oral and intravenous administration of contrast material, demonstrates ascites (*), free intraperitoneal air (arrow), and thick-walled bowel (arrowhead).

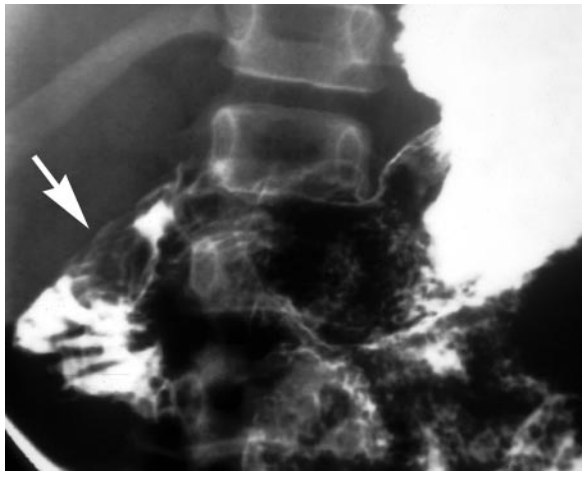

Figure 32. Duodenal hematoma in a 6-year-old boy who was beaten by a caretaker. Image from a barium study of the stomach and duodenum reveals a mass (arrow) in the lateral wall of the descending duodenum.

Small Bowel Injury

The most commonly injured abdominal organ in child abuse is the small bowel (16,186). Hematomas, lacerations, mesenteric injury, and posttraumatic stricture are all frequently reported in the

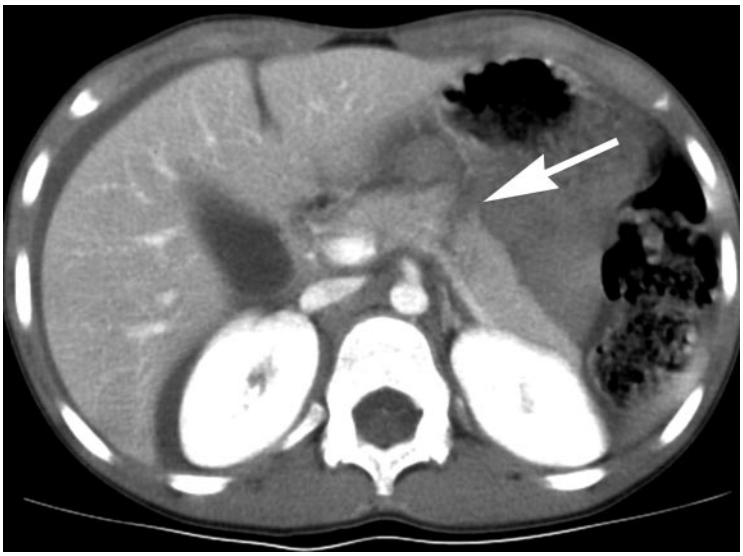

Figure 33. Pancreatic laceration in a 2-year-old girl who was beaten by a caretaker. Axial CT scan of the upper abdomen, obtained after intravenous administration of contrast material, reveals a linear defect (arrow) in the ventral body of the pancreas and generalized abdominal and retroperitoneal ascites.

literature as a result of inflicted injury (85,188–194). All these injuries tend to occur in the duodenum and proximal jejunum. This is thought to be due to the rich vascular supply of the duodenum (where hematoma predominates) and the relatively fixed position of this portion of the small bowel (with perforation predominant in the jejunum). Both blunt abdominal trauma and acute deceleration of the abdomen are theorized to cause most of the intestinal injuries in these children.

With intestinal perforation, the child presents clinically with pain and fever. Plain radiography and CT may demonstrate free intraperitoneal air, although it is not an invariable finding and was documented at CT in only 33% of cases in one study. When present, free air is highly specific for bowel perforation (Fig 31). Ascites is the most common finding at CT; it may be the result of bleeding, peritonitis, or other abdominal injury such as pancreatitis (188,195,196). Children with hematoma of the bowel wall present most often with pain and vomiting from obstruction. At barium upper gastrointestinal studies or CT, a submucosal mass is evident (usually on the lateral wall of the descending duodenum) (Fig 32). As the hematoma resolves, the mass becomes smaller and is replaced by fold thickening, which may be smooth or nodular (16). At CT, hematoma manifests as a high-attenuation mural mass, which diminishes in attenuation over time (188,195). Hematomas have been documented sonographically, appearing as hyperechoic masses initially, transitioning to mixed echogenic masses, and appearing finally as hypoechoic masses over days to weeks (197,198).

Pancreatic Injury

In children, trauma is the leading cause of pancreatitis and pancreatic pseudocyst, and it is estimated that one-third of all posttraumatic pancreatitis is abuse-related (199–201). Children present with vomiting, fever, and elevated serum levels of amylase. Pancreatitis and pseudocyst are best imaged with US and CT, which show an enlarged pancreas that is hypoechoic at US and hypoattenuating at CT (199–203). In one of the largest series of pediatric pancreatitis, the pancreas appeared normal at CT in 71% of patients. Extrapancreatic fluid was the most common imaging finding (50% of patients), which predominated in the anterior pararenal space (71%), the lesser sac (57%), and the lesser omentum (50%). Intrapancreatic fluid collections in childhood pancreatitis were distinctly unusual, discovered in only 7% of patients (204). Pancreatic transection has also been observed in abusive injury (Fig 33) (205).

Other Visceral Injuries

Injuries in virtually all sites in the human body have been seen in abused children. Lacerations, contusions, and rupture of the stomach, liver, spleen, adrenal gland, kidney, bladder, colon, esophagus, and pharynx have been described (Fig 34) (188,189,206–210). In the thorax, lung contusion, pleural effusion, cardiac laceration, and fatal commotio cordis have also been described (11,211–214). Any injury pattern may occur in child abuse, although none in the viscera is as specific for abusive injury as is the CML or posterior rib fracture in the skeleton. Therefore, careful consideration of the given history and evidence of any delay in seeking treatment are critical to discovery of abusive injury.

Conclusions

Child physical abuse is an unfortunately common occurrence that may manifest as a clinically inapparent metaphyseal fracture or as a devastating neurologic injury. Every part of the human body may be injured intentionally. Some patterns of injury (CML, posterior rib fracture, interhemispheric extraaxial hemorrhage) are highly suggestive of abuse; many more are not. Thus, careful observation of radiologic findings and their correlation with the proposed mechanism of injury and with the developmental capabilities and clinical status of the child are imperative in the evaluation of any child, lest we overlook an important clue to the inflicted nature of an injury and return a child to an abusive environment, with potentially disastrous consequences.

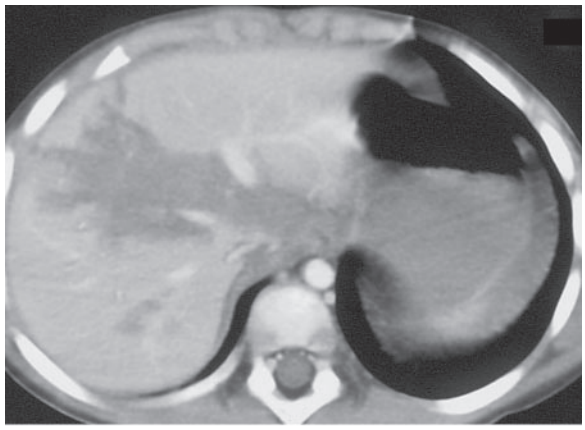

a.

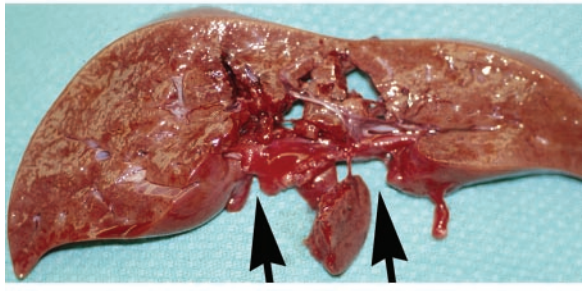

b.

Figure 34. Liver lacerations in abused children. **(a)** Axial CT scan of the liver, obtained with intravenous contrast material, in an abused 14-month-old boy demonstrates a large irregular area of low attenuation in the right lobe of the liver, representing a liver laceration. **(b)** Photograph of an axially sectioned liver from a fatally abused 8-month-old boy shows a large central laceration (arrows).

References

1. U.S. Department of Health and Human Services Children's Bureau (online). Child maltreatment 2000: reports from the states to the National Child Abuse and Neglect Data System. Available at: *http://www.calib.com/nccanch/prevmnth/scope/ncands/cfm.* Accessed February 5, 2003.
2. MacLeod J, Nelson G. Programs for the promotion of family wellness and the prevention of child maltreatment: a meta-analytic review. Child Abuse Negl 2000; 24:1127–1149.
3. Tardieu A. Etude medico-legale sur les services et mauvais traitments exerces sur des infants. Ann Hyg Publ Med Leg 1860; 13:361–398.
4. Caffey J. Multiple fractures in the long bones of infants suffering from chronic subdural hematoma. Am J Roentgenol Radium Ther Nucl Med 1946; 56:163–173.
5. Caffey J. Some traumatic lesions in growing bones other than fractures and dislocations: clinical and radiological features. Br J Radiol 1957; 30:225–238.
6. Kempe CH, Silverman FN, Steele BF, Droegemueller W, Silver HK. The battered-child syndrome. JAMA 1962; 181:105–112.
7. Guthkelch AN. Infantile subdural haematoma and its relationship to whiplash injuries. Br Med J 1971; 2:430–431.
8. Kleinman PK, Marks SC, Blackbourne B. The metaphyseal lesion in abused infants: a radiologic-histopathologic study. AJR Am J Roentgenol 1986; 146:895–905.
9. Kleinman PK, Marks SC Jr, Richmond JM, Blackbourne BD. Inflicted skeletal injury: a postmortem radiologic-histopathologic study in 31 infants. AJR Am J Roentgenol 1995; 165:647–650.
10. Kleinman PK, Marks SC Jr, Spevak MR, Belanger PL, Richmond JM. Extension of growth-plate cartilage into the metaphysis: a sign of healing fracture in abused infants. AJR Am J Roentgenol 1991; 156: 775–779.
11. Kleinman PK, Raptopoulos VD, Brill PW. Occult nonskeletal trauma in the battered-child syndrome. Radiology 1981; 141:393–396.
12. Kleinman PK, Marks SC Jr. A regional approach to the classic metaphyseal lesion in abused infants: the proximal humerus. AJR Am J Roentgenol 1996; 167:1399–1403.
13. Kleinman PK, Marks SC Jr. A regional approach to classic metaphyseal lesions in abused infants: the distal tibia. AJR Am J Roentgenol 1996; 166:1207–1212.

14. Kleinman PK, Marks SC Jr. A regional approach to the classic metaphyseal lesion in abused infants: the proximal tibia. AJR Am J Roentgenol 1996; 166: 421–426.
15. Kleinman PK, Marks SC Jr. A regional approach to the classic metaphyseal lesion in abused infants: the distal femur. AJR Am J Roentgenol 1998; 170:43–47.
16. Kleinman PK, Brill PW, Winchester P. Resolving duodenal-jejunal hematoma in abused children. Radiology 1986; 160:747–750.
17. Kleinman PK, Marks SC. Vertebral body fractures in child abuse: radiologic-histopathologic correlates. Invest Radiol 1992; 27:715–722.
18. Herndon WA. Child abuse in a military population. J Pediatr Orthop 1983; 3:73–76.
19. Akbarnia B, Torg JS, Kirkpatrick J, Sussman S. Manifestations of the battered-child syndrome. J Bone Joint Surg Am 1974; 56:1159–1166.
20. Ebbin AJ, Gollub MH, Stein AM, Wilson MG. Battered child syndrome at the Los Angeles County General Hospital. Am J Dis Child 1969; 118:660–667.
21. King J, Diefendorf D, Apthorp J, Negrete VF, Carlson M. Analysis of 429 fractures in 189 battered children. J Pediatr Orthop 1988; 8:585–589.
22. Worlock P, Stower M, Barbor P. Patterns of fractures in accidental and non-accidental injury in children: a comparative study. Br Med J (Clin Res Ed) 1986; 293:100–102.
23. Alexander CJ. Effect of growth rate on the strength of the growth plate shaft junction. Skeletal Radiol 1976; 1:67–76.
24. Merten DF, Radkowski MA, Leonidas JC. The abused child: a radiological reappraisal. Radiology 1983; 146:377–381.
25. Loder RT, Bookout C. Fracture patterns in battered children. J Orthop Trauma 1991; 5:428–433.
26. DeLee JC, Wilkins KE, Rogers LF, Rockwood CA. Fracture-separation of the distal humeral epiphysis. J Bone Joint Surg Am 1980; 62:46–51.
27. Maresh MM. Linear growth of long bones of extremities from infancy through adolescence. Am J Dis Child 1955; 89:725–742.
28. Trueta J, Amato VP. The vascular contribution to osteogenesis. III. Changes in the growth cartilage caused by experimentally induced ischaemia. J Bone Joint Surg Br 1960; 42:571–587.
29. Osier LK, Marks SC Jr, Kleinman PK. Metaphyseal extensions of hypertrophied chondrocytes in abused infants indicate healing fractures. J Pediatr Orthop 1993; 13:249–254.
30. Conway JJ, Collins M, Tanz RR, et al. The role of bone scintigraphy in detecting child abuse. Semin Nucl Med 1993; 23:321–333.
31. American Academy of Pediatrics, Section on Radiology. Diagnostic imaging of child abuse. Pediatrics 2000; 105:1345–1348.
32. Thomas PS. Rib fractures in infancy. Ann Radiol (Paris) 1977; 20:115–122.
33. Garcia VF, Gottschall CS, Eichelberger MR, Bowman LM. Rib fractures in children: a marker of severe trauma. J Trauma 1990; 30:695–700.
34. Feldman KW, Brewer DK. Child abuse, cardiopulmonary resuscitation, and rib fractures. Pediatrics 1984; 73:339–342.
35. Kleinman PK. Bony thoracic trauma. In: Kleinman PK, ed. Diagnostic imaging of child abuse. 2nd ed. St Louis, Mo: Mosby, 1998; 110–111.
36. Ng CS, Hall CM. Costochondral junction fractures and intra-abdominal trauma in non-accidental injury (child abuse). Pediatr Radiol 1998; 28:671–676.
37. Strouse PJ, Owings CL. Fractures of the first rib in child abuse. Radiology 1995; 197:763–765.
38. Hartmann RW Jr. Radiological case of the month. Rib fractures produced by birth trauma. Arch Pediatr Adolesc Med 1997; 151:947–948.
39. Rizzolo PJ, Coleman PR. Neonatal rib fracture: birth trauma or child abuse? J Fam Pract 1989; 29: 561–563.
40. Bhat BV, Kumar A, Oumachigui A. Bone injuries during delivery. Indian J Pediatr 1994; 61:401–405.
41. Kleinman PK, Marks SC, Adams VI, Blackbourne BD. Factors affecting visualization of posterior rib fractures in abused infants. AJR Am J Roentgenol 1988; 150:635–638.
42. Kleinman PK, Marks SC, Spevak MR, Richmond JM. Fractures of the rib head in abused infants. Radiology 1992; 185:119–123.
43. Kleinman PK, Schlesinger AE. Mechanical factors associated with posterior rib fractures: laboratory and case studies. Pediatr Radiol 1997; 27:87–91.
44. Kleinman PK, Marks SC Jr, Nimkin K, Rayder SM, Kessler SC. Rib fractures in 31 abused infants: postmortem radiologic-histopathologic study. Radiology 1996; 200:807–810.
45. Potts WJ. The role of the hematoma in fracture healing. Surg Gynecol Obstet 1933; 57:318–324.
46. Ham AW. A histological study of the early phases of bone repair. J Bone Joint Surg Am 1930; 12:827–844.
47. Cruess RL, Dumont J. Fracture healing. Can J Surg 1975; 18:403–413.
48. Frost HM. The biology of fracture healing: an overview for clinicians—part I. Clin Orthop 1989; Nov: 283–293.
49. Frost HM. The biology of fracture healing: an overview for clinicians—part II. Clin Orthop 1989; Nov: 294–309.
50. Kleinman PK, Nimkin K, Spevak MR, et al. Follow-up skeletal surveys in suspected child abuse. AJR Am J Roentgenol 1996; 167:893–896.
51. Sty JR, Starshak RJ. The role of bone scintigraphy in the evaluation of the suspected abused child. Radiology 1983; 146:369–375.
52. Smith FW, Gilday DL, Ash JM, Green MD. Unsuspected costo-vertebral fractures demonstrated by bone scanning in the child abuse syndrome. Pediatr Radiol 1980; 10:103–106.
53. Haase GM, Ortiz VN, Sfakianakis GN, Morse TS. The value of radionuclide bone scanning in the early recognition of deliberate child abuse. J Trauma 1980; 20:873–875.
54. Kleinman PK. Bony thoracic trauma. In: Kleinman PK, ed. Diagnostic imaging of child abuse. 2nd ed. St Louis, Mo: Mosby, 1998; 132.
55. Patterson RH, Burns WA, Jannotta FS. Complications of external cardiac resuscitation: a retrospective review and survey of the literature. Med Ann Dist Columbia 1974; 43:389–394.
56. Feldman KW, Brewer DK. Child abuse, cardiopulmonary resuscitation, and rib fractures. Pediatrics 1984; 73:339–342.
57. Bush CM, Jones JS, Cohle SD, Johnson H. Pediatric injuries from cardiopulmonary resuscitation. Ann Emerg Med 1996; 28:40–44.
58. Spevak MR, Kleinman PK, Belanger PL, Primack C, Richmond JM. Cardiopulmonary resuscitation and rib fractures in infants: a postmortem radiologic-pathologic study. JAMA 1994; 272:617–618.

59. Betz P, Liebhardt E. Rib fractures in children: resuscitation or child abuse? Int J Legal Med 1994; 106: 215–218.
60. Cumming WA. Neonatal skeletal fractures: birth trauma or child abuse? J Can Assoc Radiol 1979; 30:30–33.
61. Islam O, Soboleski D, Symons S, Davidson LK, Ashworth MA, Babyn P. Development and duration of radiographic signs of bone healing in children. AJR Am J Roentgenol 2000; 175:75–78.
62. Helfer RE, Slovis TL, Black M. Injuries resulting when small children fall out of bed. Pediatrics 1977; 60:533–535.
63. Nimityongskul P, Anderson LD. The likelihood of injuries when children fall out of bed. J Pediatr Orthop 1987; 7:184–186.
64. Lyons TJ, Oates RK. Falling out of bed: a relatively benign occurrence. Pediatrics 1993; 92:125–127.
65. Joffe M, Ludwig S. Stairway injuries in children. Pediatrics 1988; 82:457–461.
66. Bertocci GE, Pierce MC, Deemer E, Aguel F. Computer simulation of stair falls to investigate scenarios in child abuse. Arch Pediatr Adolesc Med 2001; 155:1008–1014.
67. Chiaviello CT, Christoph RA, Bond GR. Stairway-related injuries in children. Pediatrics 1994; 94:679–681.
68. Huntimer CM, Muret-Wagstaff S, Leland NL. Can falls on stairs result in small intestine perforations? Pediatrics 2000; 106:301–305.
69. Injuries associated with infant walkers. Pediatrics 2001; 108:790–792.
70. Gross RH, Davidson R, Sullivan JA, Peeples RE, Hufft R. Cast brace management of the femoral shaft fracture in children and young adults. J Pediatr Orthop 1983; 3:572–582.
71. Thomas SA, Rosenfield NS, Leventhal JM, Markowitz RI. Long-bone fractures in young children: distinguishing accidental injuries from child abuse. Pediatrics 1991; 88:471–476.
72. Swischuk LE. Spine and spinal cord trauma in the battered child syndrome. Radiology 1969; 92:733–738.
73. Kleinman PK, Zito JL. Avulsion of the spinous processes caused by infant abuse. Radiology 1984; 151: 389–391.
74. Kleinman PK, Blackbourne BD, Marks SC, Karellas A, Belanger PL. Radiologic contributions to the investigation and prosecution of cases of fatal infant abuse. N Engl J Med 1989; 320:507–511.
75. Bruce DA, Zimmerman RA. Shaken impact syndrome. Pediatr Ann 1989; 18:482–484, 486–489, 492–494.
76. Billmire ME, Myers PA. Serious head injury in infants: accident or abuse? Pediatrics 1985; 75:340–342.
77. Duhaime AC, Alario AJ, Lewander WJ, et al. Head injury in very young children: mechanisms, injury types, and ophthalmologic findings in 100 hospitalized patients younger than 2 years of age. Pediatrics 1992; 90:179–185.
78. Ludwig S, Warman M. Shaken baby syndrome: a review of 20 cases. Ann Emerg Med 1984; 13:104–107.
79. Alexander RC, Schor DP, Smith WL Jr. Magnetic resonance imaging of intracranial injuries from child abuse. J Pediatr 1986; 109:975–979.
80. Conway EE Jr. Nonaccidental head injury in infants: "the shaken baby syndrome revisited." Pediatr Ann 1998; 27:677–690.
81. Duhaime AC, Christian C, Moss E, Seidl T. Long-term outcome in infants with the shaking-impact syndrome. Pediatr Neurosurg 1996; 24:292–298.
82. Zimmerman RA, Bilaniuk LT, Bruce D, Schut L, Uzzell B, Goldberg HI. Computed tomography of craniocerebral injury in the abused child. Radiology 1979; 130:687–690.
83. Tsai FY, Zee CS, Apthorp JS, Dixon GH. Computed tomography in child abuse head trauma. J Comput Tomogr 1980; 4:277–286.
84. Merten DF, Osborne DR, Radkowski MA, Leonidas JC. Craniocerebral trauma in the child abuse syndrome: radiological observations. Pediatr Radiol 1984; 14:272–277.
85. O'Neill JA Jr, Meacham WF, Griffin JP, Sawyers JL. Patterns of injury in the battered child syndrome. J Trauma 1973; 13:332–339.
86. Cohen RA, Kaufman RA, Myers PA, Towbin RB. Cranial computed tomography in the abused child with head injury. AJR Am J Roentgenol 1986; 146: 97–102.
87. Williams RA. Injuries in infants and small children resulting from witnessed and corroborated free falls. J Trauma 1991; 31:1350–1352.
88. Tarantino CA, Dowd MD, Murdock TC. Short vertical falls in infants. Pediatr Emerg Care 1999; 15: 5–8.
89. Claydon SM. Fatal extradural hemorrhage following a fall from a baby bouncer. Pediatr Emerg Care 1996; 12:432–434.
90. Selbst SM, Baker MD, Shames M. Bunk bed injuries. Am J Dis Child 1990; 144:721–723.
91. Mayr JM, Seebacher U, Lawrenz K, Pesendorfer P, Berghold A, Baradaran S. Bunk beds: a still underestimated risk for accidents in childhood? Eur J Pediatr 2000; 159:440–443.
92. Kleinman PK, Spevak MR. Soft tissue swelling and acute skull fractures. J Pediatr 1992; 121:737–739.
93. Block RW. Child abuse: controversies and impostors. Curr Probl Pediatr 1999; 29:249–272.
94. Barnes PD, Robson CD. CT findings in hyperacute nonaccidental brain injury. Pediatr Radiol 2000; 30:74–81.
95. Meservy CJ, Towbin R, McLaurin RL, Myers PA, Ball W. Radiographic characteristics of skull fractures resulting from child abuse. AJR Am J Roentgenol 1987; 149:173–175.
96. Hobbs CJ. Skull fracture and the diagnosis of abuse. Arch Dis Child 1984; 59:246–252.
97. Saulsbury FT, Alford BA. Intracranial bleeding from child abuse: the value of skull radiographs. Pediatr Radiol 1982; 12:175–178.
98. Nimkin K, Kleinman PK. Imaging of child abuse. Radiol Clin North Am 2001; 39:843–864.
99. Shugerman RP, Paez A, Grossman DC, Feldman KW, Grady MS. Epidural hemorrhage: is it abuse? Pediatrics 1996; 97:664–668.
100. Reece RM, Sege R. Childhood head injuries: accidental or inflicted? Arch Pediatr Adolesc Med 2000; 154:11–15.
101. Dashti SR, Decker DD, Razzaq A, Cohen AR. Current patterns of inflicted head injury in children. Pediatr Neurosurg 1999; 31:302–306.
102. Holden KR, Titus MO, Van Tassel P. Cranial magnetic resonance imaging examination of normal term neonates: a pilot study. J Child Neurol 1999; 14:708–710.
103. Zimmerman RA, Tavani F, Mahle WS, Clancy RR. Incidence of subdural hemorrhage by MR in term neonates with congenital heart disease undergoing vaginal delivery. Presented at the 45th Annual Meeting of the Society for Pediatric Radiology, Philadelphia, April 28–May 1, 2002.

104. Zimmerman RA, Bilaniuk LT. Pediatric head trauma. Neuroimaging Clin N Am 1994; 4:349–366.
105. Sato Y, Yuh WT, Smith WL, Alexander RC, Kao SC, Ellerbroek CJ. Head injury in child abuse: evaluation with MR imaging. Radiology 1989; 173: 653–657.
106. Zimmerman RA, Bilaniuk LT, Bruce D, Schut L, Uzzell B, Goldberg HI. Interhemispheric acute subdural hematoma: a computed tomographic manifestation of child abuse by shaking. Neuroradiology 1978; 16:39–40.
107. Zimmerman RD, Russell EJ, Yurberg E, Leeds NE. Falx and interhemispheric fissure on axial CT. II. Recognition and differentiation of interhemispheric subarachnoid and subdural hemorrhage. AJNR Am J Neuroradiol 1982; 3:635–642.
108. Ommaya AK, Yarnell P. Subdural haematoma after whiplash injury. Lancet 1969; 2:237–239.
109. Chen JC, Levy ML. Causes, epidemiology, and risk factors of chronic subdural hematoma. Neurosurg Clin N Am 2000; 11:399–406.
110. Maxeiner H. Demonstration and interpretation of bridging vein ruptures in cases of infantile subdural bleedings. J Forensic Sci 2001; 46:85–93.
111. Friede RL, Schachenmayr W. The origin of subdural neomembranes. II. Fine structural of neomembranes. Am J Pathol 1978; 92:69–84.
112. Frederickson RG. The subdural space interpreted as a cellular layer of meninges. Anat Rec 1991; 230: 38–51.
113. Killeffer JA, Killeffer FA, Schochet SS. The outer neomembrane of chronic subdural hematoma. Neurosurg Clin N Am 2000; 11:407–412.
114. Yamashima T, Friede RL. Why do bridging veins rupture into the virtual subdural space? J Neurol Neurosurg Psychiatry 1984; 47:121–127.
115. Schachenmayr W, Friede RL. The origin of subdural neomembranes. I. Fine structure of the dura-arachnoid interface in man. Am J Pathol 1978; 92: 53–68.
116. Yamashima T. The inner membrane of chronic subdural hematomas: pathology and pathophysiology. Neurosurg Clin N Am 2000; 11:413–424.
117. Duhaime AC, Christian CW, Rorke LB, Zimmerman RA. Nonaccidental head injury in infants: the "shaken-baby syndrome." N Engl J Med 1998; 338: 1822–1829.
118. Case ME, Graham MA, Handy TC, Jentzen JM, Monteleone JA. Position paper on fatal abusive head injuries in infants and young children. Am J Forensic Med Pathol 2001; 22:112–122.
119. Ikeda K, Ito H, Yamashita J. Relation of regional cerebral blood flow to hemiparesis in chronic subdural hematoma. Surg Neurol 1990; 33:87–95.
120. Munro DM. Surgical pathology of subdural hematoma: based on a study of one hundred and five cases. Arch Neurol Psychol 1936; 35:64–78.
121. Sato S, Suzuki J. Ultrastructural observations of the capsule of chronic subdural hematoma in various clinical stages. J Neurosurg 1975; 43:569–578.
122. Suzuki K, Sugita K, Akai T, Takahata T, Sonobe M, Takahashi S. Treatment of chronic subdural hematoma by closed-system drainage without irrigation. Surg Neurol 1998; 50:231–234.
123. Yamashima T, Yamamoto S, Friede RL. The role of endothelial gap junctions in the enlargement of chronic subdural hematomas. J Neurosurg 1983; 59:298–303.
124. Murakami H, Hirose Y, Sagoh M, et al. Why do chronic subdural hematomas continue to grow slowly and not coagulate? Role of thrombomodulin in the mechanism. J Neurosurg 2002; 96:877–884.
125. Ito H, Komai T, Yamamoto S. Fibrinolytic enzyme in the lining walls of chronic subdural hematoma. J Neurosurg 1978; 48:197–200.
126. Lim DJ, Chung YG, Park YK, et al. Relationship between tissue plasminogen activator, plasminogen activator inhibitor and CT image in chronic subdural hematoma. J Korean Med Sci 1995; 10:373–378.
127. Hardman JM. The pathology of traumatic brain injuries. Adv Neurol 1979; 22:15–50.
128. Bergstrom M, Ericson K, Levander B, Svendsen P. Computed tomography of cranial subdural and epidural hematomas: variation of attenuation related to time and clinical events such as rebleeding. J Comput Assist Tomogr 1977; 1:449–455.
129. Lee KS, Bae WK, Bae HG, Doh JW, Yun IG. The computed tomographic attenuation and the age of subdural hematomas. J Korean Med Sci 1997; 12: 353–359.
130. Dias MS, Backstrom J, Falk M, Li V. Serial radiography in the infant shaken impact syndrome. Pediatr Neurosurg 1998; 29:77–85.
131. Kao MC. Sedimentation level in chronic subdural hematoma visible on computerized tomography. J Neurosurg 1983; 58:246–251.
132. Scotti G, Terbrugge K, Melancon D, Belanger G. Evaluation of the age of subdural hematomas by computerized tomography. J Neurosurg 1977; 47: 311–315.
133. Firsching R, Frowein RA, Thun F. Encapsulated subdural hematoma. Neurosurg Rev 1989; 12(suppl 1):207–214.
134. Sargent S, Kennedy JG, Kaplan JA. "Hyperacute" subdural hematoma: CT mimic of recurrent episodes of bleeding in the setting of child abuse. J Forensic Sci 1996; 41:314–316.
135. Greenberg J, Cohen WA, Cooper PR. The "hyperacute" extraaxial intracranial hematoma: computed tomographic findings and clinical significance. Neurosurgery 1985; 17:48–56.
136. Ikeda A, Sato O, Tsugane R, Shibuya N, Yamamoto I, Shimoda M. Infantile acute subdural hematoma. Childs Nerv Syst 1987; 3:19–22.
137. Bradley WG Jr. MR appearance of hemorrhage in the brain. Radiology 1993; 189:15–26.
138. Kleinman PK, Ragland RL. Gadopentetate dimeglumine-enhanced MR imaging of subdural hematoma in an abused infant. AJR Am J Roentgenol 1996; 166:1456–1458.
139. Chen CY, Huang CC, Zimmerman RA, et al. High-resolution cranial ultrasound in the shaken-baby syndrome. Neuroradiology 2001; 43:653–661.
140. Kleinman PK, Barnes PD. Head trauma. In: Kleinman PK, ed. Diagnostic imaging of child abuse. 2nd ed. St Louis, Mo: Mosby, 1998; 306–307.
141. Krous HF, Byard RW. Shaken infant syndrome: selected controversies. Pediatr Dev Pathol 1999; 2:497–498.
142. Kirschner RH. The pathology of child abuse. In: Helfer ME, Kempe RS, Krugman RD, eds. The battered child. 5th ed. Chicago, Ill: University of Chicago Press, 1998; 271–274.
143. Holbourn AH. Mechanics of head injuries. Lancet 1943; 2:438–441.
144. Holbourn AH. The mechanics of brain injury. Br Med Bull 1945; 3:147–149.
145. Calder IM, Hill I, Scholtz CL. Primary brain trauma in non-accidental injury. J Clin Pathol 1984; 37:1095–1100.
146. Vowles GH, Scholtz CL, Cameron JM. Diffuse axonal injury in early infancy. J Clin Pathol 1987; 40: 185–189.

147. Lindenberg R, Freytag E. Morphology of brain lesions from blunt trauma in early infancy. Arch Pathol 1969; 87:298–305.
148. Adams JH, Graham DI, Murray LS, Scott G. Diffuse axonal injury due to nonmissile head injury in humans: an analysis of 45 cases. Ann Neurol 1982; 12:557–563.
149. Shannon P, Smith CR, Deck J, Ang LC, Ho M, Becker L. Axonal injury and the neuropathology of shaken baby syndrome. Acta Neuropathol (Berl) 1998; 95:625–631.
150. McKenzie KJ, McLellan DR, Gentleman SM, Maxwell WL, Gennarelli TA, Graham DI. Is beta-APP a marker of axonal damage in short-surviving head injury? Acta Neuropathol (Berl) 1996; 92:608–613.
151. Gentleman SM, Nash MJ, Sweeting CJ, Graham DI, Roberts GW. Beta-amyloid precursor protein (beta APP) as a marker for axonal injury after head injury. Neurosci Lett 1993; 160:139–144.
152. Kaur B, Rutty GN, Timperley WR. The possible role of hypoxia in the formation of axonal bulbs. J Clin Pathol 1999; 52:203–209.
153. Geddes JF, Hackshaw AK, Vowles GH, Nickols CD, Whitwell HL. Neuropathology of inflicted head injury in children. I. Patterns of brain damage. Brain 2001; 124:1290–1298.
154. Geddes JF, Vowles GH, Hackshaw AK, Nickols CD, Scott IS, Whitwell HL. Neuropathology of inflicted head injury in children. II. Microscopic brain injury in infants. Brain 2001; 124:1299–1306.
155. Johnson DL, Boal D, Baule R. Role of apnea in nonaccidental head injury. Pediatr Neurosurg 1995; 23:305–310.
156. Auer RN. Hypoxia and related conditions. London, England: Arnold, 2002.
157. Kleinman PK, Barnes PD. Head trauma. In: Kleinman PK, ed. Diagnostic imaging of child abuse. 2nd ed. St Louis, Mo: Mosby, 1998; 316.
158. Kleinman PK, Barnes PD. Head trauma. In: Kleinman PK, ed. Diagnostic imaging of child abuse. 2nd ed. St Louis, Mo: Mosby, 1998; 317.
159. Jaspan T, Narborough G, Punt JA, Lowe J. Cerebral contusional tears as a marker of child abuse: detection by cranial sonography. Pediatr Radiol 1992; 22:237–245.
160. Duhaime AC, Gennarelli TA, Thibault LE, Bruce DA, Margulies SS, Wiser R. The shaken baby syndrome: a clinical, pathological, and biomechanical study. J Neurosurg 1987; 66:409–415.
161. Kleinman PK, Barnes PD. Head trauma. In: Kleinman PK, ed. Diagnostic imaging of child abuse. 2nd ed. St Louis, Mo: Mosby, 1998; 315.
162. Chen CY, Zimmerman RA, Rorke LB. Neuroimaging in child abuse: a mechanism-based approach. Neuroradiology 1999; 41:711–722.
163. Hadley MN, Sonntag VK, Rekate HL, Murphy A. The infant whiplash-shake injury syndrome: a clinical and pathological study. Neurosurgery 1989; 24: 536–540.
164. Gleckman AM, Bell MD, Evans RJ, Smith TW. Diffuse axonal injury in infants with nonaccidental craniocerebral trauma: enhanced detection by beta-amyloid precursor protein immunohistochemical staining. Arch Pathol Lab Med 1999; 123:146–151.
165. Geddes JF, Whitwell HL, Graham DI. Traumatic axonal injury: practical issues for diagnosis in medicolegal cases. Neuropathol Appl Neurobiol 2000; 26:105–116.
166. Suh DY, Davis PC, Hopkins KL, Fajman NN, Mapstone TB. Nonaccidental pediatric head injury: diffusion-weighted imaging findings. Neurosurgery 2001; 49:309–318; discussion 318–320.
167. Biousse V, Suh DY, Newman NJ, Davis PC, Mapstone T, Lambert SR. Diffusion-weighted magnetic resonance imaging in shaken baby syndrome. Am J Ophthalmol 2002; 133:249–255.
168. Han BK, Towbin RB, De Courten-Myers G, McLaurin RL, Ball WS Jr. Reversal sign on CT: effect of anoxic/ischemic cerebral injury in children. AJR Am J Roentgenol 1990; 154:361–368.
169. Harwood-Nash DC. Abuse to the pediatric central nervous system. AJNR Am J Neuroradiol 1992; 13: 569–575.
170. Schaefer PW, Grant PE, Gonzalez RG. Diffusion-weighted MR imaging of the brain. Radiology 2000; 217:331–345.
171. Liu AY, Maldjian JA, Bagley LJ, Sinson GP, Grossman RI. Traumatic brain injury: diffusion-weighted MR imaging findings. AJNR Am J Neuroradiol 1999; 20:1636–1641.
172. Ommaya AK, Faas F, Yarnell P. Whiplash injury and brain damage: an experimental study. JAMA 1968; 204:285–289.
173. Caffey J. The whiplash shaken infant syndrome: manual shaking by the extremities with whiplash-induced intracranial and intraocular bleedings, linked with residual permanent brain damage and mental retardation. Pediatrics 1974; 54:396–403.
174. Ommaya AK, Goldsmith W, Thibault L. Biomechanics and neuropathology of adult and paediatric head injury. Br J Neurosurg 2002; 16:220–242.
175. Zhang L, Yang KH, King AI. Biomechanics of neurotrauma. Neurol Res 2001; 23:144–156.
176. Gilliland MG, Luckenbach MW, Chenier TC. Systemic and ocular findings in 169 prospectively studied child deaths: retinal hemorrhages usually mean child abuse. Forensic Sci Int 1994; 68:117–132.
177. Morad Y, Kim YM, Armstrong DC, Huyer D, Mian M, Levin AV. Correlation between retinal abnormalities and intracranial abnormalities in the shaken baby syndrome. Am J Ophthalmol 2002; 134:354–359.
178. Alexander R, Sato Y, Smith W, Bennett T. Incidence of impact trauma with cranial injuries ascribed to shaking. Am J Dis Child 1990; 144:724–726.
179. Gilliland MG, Folberg R. Shaken babies: some have no impact injuries. J Forensic Sci 1996; 41:114–116.

180. Pounder DJ. Shaken adult syndrome. Am J Forensic Med Pathol 1997; 18:321–324.
181. Elder JE, Taylor RG, Klug GL. Retinal haemorrhage in accidental head trauma in childhood. J Paediatr Child Health 1991; 27:286–289.
182. Ewing-Cobbs L, Prasad M, Kramer L, et al. Acute neuroradiologic findings in young children with inflicted or noninflicted traumatic brain injury. Childs Nerv Syst 2000; 16:25–33.
183. DiScala C, Sege R, Li G, Reece RM. Child abuse and unintentional injuries: a 10-year retrospective. Arch Pediatr Adolesc Med 2000; 154:16–22.
184. Kivlin JD, Simons KB, Lazoritz S, Ruttum MS. Shaken baby syndrome. Ophthalmology 2000; 107: 1246–1254.
185. Feldman KW, Weinberger E, Milstein JM, Fligner CL. Cervical spine MRI in abused infants. Child Abuse Negl 1997; 21:199–205.
186. Kirks DR. Radiological evaluation of visceral injuries in the battered child syndrome. Pediatr Ann 1983; 12:888–893.
187. Ng CS, Hall CM, Shaw DG. The range of visceral manifestations of non-accidental injury. Arch Dis Child 1997; 77:167–174.
188. Sivit CJ, Taylor GA, Eichelberger MR. Visceral injury in battered children: a changing perspective. Radiology 1989; 173:659–661.
189. Cooper A, Floyd T, Barlow B, et al. Major blunt abdominal trauma due to child abuse. J Trauma 1988; 28:1483–1487.
190. Ledbetter DJ, Hatch EI Jr, Feldman KW, Fligner CL, Tapper D. Diagnostic and surgical implications of child abuse. Arch Surg 1988; 123:1101–1105.
191. Touloukian RJ. Abdominal visceral injuries in battered children. Pediatrics 1968; 42:642–646.
192. McCort J, Vaudagna J. Visceral injuries in battered children. Radiology 1964; 82:424–428.
193. Woolley MM, Mahour GH, Sloan T. Duodenal hematoma in infancy and childhood: changing etiology and changing treatment. Am J Surg 1978; 136:8–14.
194. Fossum RM, Descheneaux KA. Blunt trauma of the abdomen in children. J Forensic Sci 1991; 36:47–50.
195. Kunin JR, Korobkin M, Ellis JH, Francis IR, Kane NM, Siegel SE. Duodenal injuries caused by blunt abdominal trauma: value of CT in differentiating perforation from hematoma. AJR Am J Roentgenol 1993; 160:1221–1223.
196. Sivit CJ, Eichelberger MR, Taylor GA. CT in children with rupture of the bowel caused by blunt trauma: diagnostic efficacy and comparison with hypoperfusion complex. AJR Am J Roentgenol 1994; 163:1195–1198.
197. Radkowski MA. The battered child syndrome: pitfalls in radiological diagnosis. Pediatr Ann 1983; 12:894–903.
198. Hernanz-Schulman M, Genieser NB, Ambrosino M. Sonographic diagnosis of intramural duodenal hematoma. J Ultrasound Med 1989; 8:273–276.
199. Cooney DR, Crosfeld JL. Operative management of pancreatic pseudocysts in infants and children: a review of 75 cases. Ann Surg 1975; 182:590–596.
200. Ziegler DW, Long JA, Philippart AI, Klein MD. Pancreatitis in childhood: experience with 49 patients. Ann Surg 1988; 207:257–261.
201. Slovis TL, Berdon WE, Haller JO, Baker DH, Rosen L. Pancreatitis and the battered child syndrome: report of 2 cases with skeletal involvement. Am J Roentgenol Radium Ther Nucl Med 1975; 125:456–461.
202. Slovis TL, VonBerg VJ, Mikelic V. Sonography in the diagnosis and management of pancreatic pseudocysts and effusions in childhood. Radiology 1980; 135:153–155.
203. Herman TE, Siegel MJ. CT of the pancreas in children. AJR Am J Roentgenol 1991; 157:375–379.
204. King LR, Siegel MJ, Balfe DM. Acute pancreatitis in children: CT findings of intra- and extrapancreatic fluid collections. Radiology 1995; 195:196–200.
205. Hilfer CL, Holgersen LO. Massive chylous ascites and transected pancreas secondary to child abuse: successful non-surgical management. Pediatr Radiol 1995; 25:117–119.
206. Case ME, Nanduri R. Laceration of the stomach by blunt trauma in a child: a case of child abuse. J Forensic Sci 1983; 28:496–501.
207. Nimkin K, Teeger S, Wallach MT, DuVally JC, Spevak MR, Kleinman PK. Adrenal hemorrhage in abused children: imaging and postmortem findings. AJR Am J Roentgenol 1994; 162:661–663.
208. Halsted CC, Shapiro SR. Child abuse: acute renal failure from ruptured bladder. Am J Dis Child 1979; 133:861–862.
209. Ablin DS, Reinhart MA. Esophageal perforation with mediastinal abscess in child abuse. Pediatr Radiol 1990; 20:524–525.
210. Kleinman PK, Spevak MR, Hansen M. Mediastinal pseudocyst caused by pharyngeal perforation during child abuse. AJR Am J Roentgenol 1992; 158:1111–1113.
211. Bongiovi JJ, Logosso RD. Pancreatic pseudocyst occurring in the battered child syndrome. J Pediatr Surg 1969; 4:220–226.
212. Cumberland GD, Riddick L, McConnell CF. Intimal tears of the right atrium of the heart due to blunt force injuries to the abdomen: its mechanism and implications. Am J Forensic Med Pathol 1991; 12:102–104.
213. Cohle SD, Hawley DA, Berg KK, Kiesel EL, Pless JE. Homicidal cardiac lacerations in children. J Forensic Sci 1995; 40:212–218.
214. Baker AM, Craig BR, Lonergan GJ. Homicidal commotio cordis: the final blow in a battered infant. Child Abuse Negl 2003; 27:125–130.

This article meets the criteria for 1.0 credit hour in category 1 of the AMA Physician's Recognition Award. To obtain credit, see accompanying test at http://www.rsna.org/education/rg_cme.html.